**University of Bath**

**Alternative formats**
If you require this document in an alternative format, please contact:
openaccess@bath.ac.uk

# Performance Of A Dynamic Cobble Berm Revetment for Coastal Protection, under increasing water level.

Paul M. Bayle, (p.m.bayle@bath.ac.uk)[a], Chris E. Blenkinsopp, (cb761@bath.ac.uk)[a], Daniel Conley, (daniel.conley@plymouth.ac.uk)[b], Gerd Masselink, (gerd.masselink@plymouth.ac.uk)[b], Tomas Beuzen, (t.beuzen@unsw.edu.au)[d], Rafael Almar, (rafael.almar@legos.obs-mip.fr)[c]

[a]*Water Environment and Infrastructure Resilience Research Unit, Department of Architecture and Civil Engineering, University of Bath, Bath, BA2 7AY, United Kingdom*
[b]*Coastal Processes Research Group, School of Biological and Marine Sciences, Plymouth University, Plymouth, UK*
[c]*LEGOS CNRS/IRD/CNES/UPS, Toulouse, France*
[d]*Water Research Laboratory, School of Civil and Environmental Engineering, UNSW Sydney, NSW, 2052, Australia*

## Abstract

In a changing climate, sea level rise and projected regional–scale changes in storminess may increase the vulnerability of sandy coastlines to coastal erosion and flooding. As a result, there is increased interest in the development of adaptable, sustainable and effective coastal protection measures to protect these highly variable sandy coastlines. One such example is a dynamic cobble berm revetment; a "soft–engineering" solution (*i.e.*, not fixed) consisting of a cobble berm constructed around the high tide wave runup limit, that has the potential to stabilise the upper beach, provide overtopping protection to the hinterland and translate with water level rise. However, there have been limited applications of dynamic cobble berm revetments to date, and there is a lack of understanding about the efficacy of this coastal protection to current and changing waves and water levels. This study details a prototype–scale experiment conducted to test the behaviour and performance of a dynamic cobble berm revetment as a form of coastal protection against erosive waves and water level increase. Results from the experiment showed that the revetment was "dynamically stable" under wave action as a consistent global shape was retained even though individual cobbles were mobilised under every swash event. Although the front slope and the crest responded to the incident wave condition, the net rate of change was always an order of magnitude lower than the gross rate of change. Tracking of individual cobbles using Radio Frequency Identification (RFID) technology showed that stability of the revetment was likely maintained by rollover transport of cobbles onto the crest, as the revetment moved upward and landward under water level rise. The presence of the revetment reduced the vertical and horizontal runup as well as the retreat of the upper beach. The experimental results presented suggest that a dynamic cobble berm revetment could be a cheap, efficient and low environmental impact engineering solution for protecting sandy coastlines in a changing climate. Some preliminary design guidelines for coastal engineers are also drawn from this experiment.

*Keywords:*
Dynamic Cobble Berm Revetment; Dynamic Revetment; Coastal adaptation; Composite beach; DynaRev

# 1. Introduction

Coastal areas are home to cultural, social and environmental assets which contribute significantly to the national economies in many countries. They are all different in terms of their geology, habitat and urbanisation characteristics and are one of the most threatened environments from climate change induced sea level rise (SLR) and increasing storm severity (DeConto & Pollard, 2016). In light of these threats, the need to protect the coast from erosion and flooding is only expected to increase and there is a need to consider new approaches to coastal management and new types of coastal structures to ensure the sustainability of our coasts.

One promising structure, with respect to its potential for adaptation to a changing climate, is a dynamic cobble berm revetment. There have been several studies examining dynamic cobble berm revetments, and related structures, in the field and in small–scale laboratory experiments (van Hijum & Pilarczyk, 1982; Downie & Saaltink, 1983; Pilarczyk & Boer, 1983; Johnson, 1987; van der Meer & Pilarczyk, 1986; Powell, 1988; Ahrens, 1990; Lorang, 1991; Ward & Ahrens, 1992; Kirk, 1992; Allan et al., 2006; Komar & Allan, 2010; Loman et al., 2010; Allan et al., 2012, 2016; Allan & Gabel, 2016). However to date, there has been no detailed study into the performance of dynamic cobble berm revetments under controlled conditions at prototype scale, and in particular under changing water levels. In this paper, we investigate the performance and resilience of a dynamic cobble berm revetment under water level changes for a range of wave conditions in a large scale laboratory flume. This work presents new information about the application of such structures for coastal protection under energetic conditions and for a rising water level.

The paper is structured as follows: Section 2 presents a background of coastal protection and a detailed literature review of existing studies and applications of dynamic cob-ble berm revetments. Section 3 details the methodology used in the large scale laboratory flume experiment undertaken to test the performance of the prototype structure. Section 4 investigates the behaviour and performance of the dynamic cobble berm revetment as a coastal defence. Section 5 discusses the results and limitations, focusing on maintenance and application of such a structure. Section 6 presents a preliminary guidance on the implementation of a dynamic cobble berm revetment as a coastal protection. Section 7 concludes the study and introduces future work.

# 2. Background and literature review

## 2.1. Coastal protection techniques

Coastal protection methods can be divided into hard and soft engineering techniques (Dean & Dalrymple, 2002; Cartwright et al., 2008; Hudson et al., 2008). Hard engineering techniques consist of building fixed structures to counteract natural processes and protect the coastline; soft engineering consists of implementing less rigid techniques which are usually integrated and work with natural processes to protect the coastline.

Hard engineering structures often have a negative impact on beach amenity and the natural landscape. From an engineering prospective, existing hard engineering structures need to be maintained to continue to provide protection under new design wave and water level conditions associated with a changing climate. Such maintenance works can be done for structures like submerged artificial reefs but can be more complex for seawalls as the foundations are not designed to withstand additional load. In all cases, such modifications are likely to be expensive. Revetment and rock armour upgrades are hard to achieve as the addition of an extra layer of material usually creates planes of weakness (Howe & Cox, 2018). Howe & Cox (2018) suggested that efficient top–up maintenance

2

could be achieved using a higher density layer, however this method is only at the prototype testing stage.

Existing hard engineering protections have rarely been designed to face extreme and long–term water level changes; thus, soft engineering could become a sustainable alternative for areas where the required level of protection does not necessitate hard engineering. Classic soft engineering techniques like beach or dune nourishment and submerged nourishment are expensive and can be destructive to the ecosystem (Seymour et al., 1995). In addition, they generally have a short life span (depends on the quantity of nourished sediment). However, because they are maintained or re–implemented at least every decade, they can be modified to cope with changes in design conditions (Dean & Dalrymple, 2002; Cartwright et al., 2008; Hudson et al., 2008; French, 2001; Sorensen, 2006).

### 2.2. Composite beach

In this paper, we investigate the performance of a "dynamic cobble berm revetment" (Figure 1b) defined here as a cobble ridge constructed around the wave runup limit on sandy beaches to mimic natural composite beaches (Jennings & Schulmeister, 2002). Composite beaches (Figure 1a) consist of a lower foreshore of sand and a backshore ridge composed of gravel or cobbles which stabilises the upper beach and provides overtopping protection to the hinterland. Like gravel beaches, they have long been recognised as an effective form of natural coastal protection (Allan et al., 2016), showing a great degree of stability and adaptability in the face of wave attack by reshaping and self maintaining their relative elevation to the water level. On composite beaches, the cobble ridge is generally exposed at all stages of the tide when the tidal range and wave conditions are small. For larger wave conditions and particularly during spring



(a)



(b)

Figure 1: (a) Photo of a natural composite beach, at Kalaloch, Washington State, the USA. Cobbles are relatively similar in shape and size to those in this study. Note that drift wood is regularly deposited on the upper part of the beach at this location. (b) Photo of the dynamic cobble berm revetment as built during the DynaRev experiment. *Photo from Paul Bayle.*

tides, the ridges are exposed to swash processes and may be overtopped during particularly energetic events (Everts et al., 2002; Allan & Komar, 2004). Unlike pure and mixed sand–gravel type of gravel beaches, composite beaches have received little attention in the literature and have not been investigated using long–term (decades) field surveys or laboratory experiments. A dynamic cobble berm revetment is designed to mimic the cobble ridge of a natural composite beach. These structures contrast with static coastal defence structures as they are dynamic and are expected to reshape under wave attack and retreat as the sea level rises.

## 2.3. Review of dynamic cobble berm revetment

The concept of a dynamic cobble berm revetment is not new, and previous research has investigated a range of structures with similarities to that explored here which have been variously termed "dynamic revetment", "cobble berms", "gravel ridge" or "artificial cobble beaches" (Lorang, 1991; Kirk, 1992; Allan et al., 2012; Allan & Gabel, 2016). In many cases however, there have been significant differences in the form and function of these structures and only a few examples of the structure type that is the subject of this paper exist.

The most recent example of what is termed here a "dynamic cobble berm revetment" was installed in North Cove, Washington State, USA in 2017. The community of North Cove has a history of rapid coastal erosion, with a 2 km length of coast eroding by around 13 m per year. In order to slow this erosion, the local population have gradually implemented a dynamic revetment composed of locally–sourced, inexpensive, poorly sorted angular material, ranging in size from $D_{50} = 1$ cm to $D_{50} = 80$ cm. The material was randomly placed in an ad hoc manner over time along the back of the beach, especially when and where the erosion sand scarp was exposed. The revetment has been seen to mitigate the effect of storm erosion and protect the hinterland (Weiner et al., 2019).

A dynamic cobble berm revetment was installed to provide coastal protection along a 300 m stretch of the highly vulnerable sandy beach of Cape Lookout State Park, Oregon, USA (Komar & Allan, 2010). The revetment was completed in December 2000, and was designed to protect the hinterland. It consisted of a ridge of cobbles backed by an artificial dune reinforced with geotextile sand bags to protect the hinterland against storm waves. Such beaches are relatively common on many coasts, so the placement of a cobble berm could be considered to be a more natural and aesthetic solution than a conventional revetment or seawall. Although the hybrid dynamic revetment/dune was not constructed to the design height to protect the hinterland against extreme winter waves and water levels by the contractors, it remained stable and provided overtopping and erosion protection for almost two decades. Over time however, longshore transport has moved cobbles northward, leading to depletion of the revetment in the southern end of the beach (Allan et al., 2006).

Another example of a dynamic cobble berm revetment was installed at the Columbia River south jetty in October 2013 to protect the foredune and prevent the spit from breaching (Allan & Gabel, 2016). The structure was constructed using 3 different layers: a bedding filter layer on the excavated sand bed using angular gravel ($D_{50} = 25$ mm); a core layer made of angular gravel ($D_{50} = 25$ mm to $D_{50} = 203$ mm), which was expected to become sub–rounded by wave action in 2–5 years; and an upper layer of rounded cobbles ($D_{50} = 25$ mm to $D_{50} = 203$ mm). The structure had a front slope of 1:5 and the crest height was set to 6.7 m based on a study of wave runup. The berm width, which was identified as a key parameter, was set to 19.8 m, in agreement with previous observations of the Cape Lookout dynamic revetment and natural gravel beaches in Oregon. The storm response of this revetment was monitored along 780 m of beach, using 28 surveyed transects 25 m to 40 m apart, with 10 monitoring campaigns from the end of its construction to September 2015. Primary analysis showed that sediment is moving slowly southward. Due to this longshore transport, maintenance work is expected to be required every 10–15 years in order to keep the revetment operational for its expected life of 30–50 years.

The oldest example of a dynamic cobble

4

berm revetment is the one installed in 1981 along 300 metres of the sand cliffs forming the westerly boundary of the University of British Columbia, Canada (Downie & Saaltink, 1983). In 1981, an artificial cobble beach was constructed over 300 m. It consisted of drift sills made of heavy boulders ($D_{50} = 1.5$ m diameter) and oriented perpendicular to the coast. They were then filled and covered with smaller cobbles ($D_{50} = 10$ cm). The structure extended from 0.6 m contour elevation up to the berm elevated to 6.4 m, with a 1:15 slope. The width of the berm extended back to the toe of the cliff talus. This flat area was also covered with sand and vegetated to satisfy the beach users. The subtidal zone was composed of natural river sand exposed at low tide. In this case, the structure goal was to protect the cliff against storm induced waves and drift logs movement, as well as retaining the talus' sand falling from the cliff. Overall, the protection was a success as it maintained the recreational area while stabilising the talus. However, the sills reduced in height by 0.6 m, and therefore, a lot of material bypassed southward. It was observed that storm waves tended to push the cobbles up to the beach, with the crest forming above the original berm level. The slope also changed from 1:15 to 1:3 during energetic conditions.

At Washdyke beach in South Canterbury, New Zealand, through a beach reconstruction and renourishment scheme, an experimental gravel ridge was constructed over a 300 m long section of coastline significantly affected by erosion, flooding and retreat (Kirk, 1992). The local beach material was first reworked and reshaped as a berm to raise the overall crest height by 2.00–2.5 m. The reformed crest was then capped by 9,800 m$^3$ of coarser river gravel which was expected to be much more resistant to erosion than the fine beach grain. The revetment was built in 1980 and monitored for 5 years. During this period,

the crest of the protected area remained static while the adjacent unprotected section experienced a retreat of 11.5 m to 22.5 m. In addition, the overall erosion rate was reduced by 55 %, and no overtopping induced flooding was recorded.

While different to the dynamic cobble berm revetments that are the focus of this paper, a variety of similar structures have been discussed in the literature. Several authors describe the installation of a full gravel beach extending below the level of Minimum Low Water Shoreline (MLWS) to protect a given asset. The few examples of application of this type are well summarised by Allan & Gabel (2016). Johnson (1987) discusses a series of artificially constructed gravel beaches which they termed "dynamic revetments" and were installed in the Great Lakes after realising that the eroded copper mine tailings naturally spread and formed a gravel beach which significantly reduced the erosion of the area.

At Flathead Lake in Montana, a perched gravel beach (Lorang, 1991) was constructed using a stable base of boulders overlain by cobbles to mitigate shoreline erosion. This type of design makes the revetment dynamic with respect to the motion of cobbles on the front slope, but the underlying boulders keep the whole structure static and prevent it from adjusting its position in the cross–shore. The structure was found to reduce erosion, but material was transported away from the protected area under oblique wave induced longshore currents.

A gravel beach (Allan et al., 2012) was installed in March 2007 at Yaquina Bay, Oregon where the erosion due to ebb and flood tide created critical damage to a path and threatened the assets of the Hatfield Marine Science Centre. The structure was installed in the north part of the area, and was shown to stabilise the shoreline and walking path. After erosive events in winter 2009–2010, an addi-

tional gravel beach was installed in November–December 2011 to stabilise the southern part of the area. The structure acted as a buffer and protected the foot path behind. It also showed a dynamic behavior with the revetment profile changing both alongshore and cross–shore while remaining fairly stable.

A gravel beach (Loman et al., 2010) was used as part of the coastal protection for the Port of Rotterdam expansion in 2008. This artificial gravel beach differs slightly from those discussed above because it is combined with a submerged artificial reef. The gravel beach was composed of a thick layer of cobbles and placed to form a typical gravel beach–dune profile (Loman et al., 2010). This approach of combining a cobble beach with an underwater breakwater was also used on the Adriatic coast of Italy, near Bari (Tomasicchio et al., 2010). A multi–layer capping composed of geotextile, calcareous gravel, local stone and cobbles was used for reclaiming contaminated coastal areas. The role of the breakwater was to decrease the wave energy reaching the coastline, while the cobble top layer of the capping was designed to dissipate the swash energy through dynamic motion.

A number of laboratory experiments have been undertaken that are relevant to the different types of dynamic revetment structure discussed above. For example, van Hijum & Pilarczyk (1982) and Pilarczyk & Boer (1983) investigated the design of artificial gravel beaches, while Powell (1988) studied the potential use of a coarse grain beach for coastal protection in place of a conventional revetment. Ahrens (1990) and Ward & Ahrens (1992) (see also Tomasicchio et al. (1994)) conducted a flume experiment to assess the performance of a coastal structure, which consisted of small rocks placed on a concrete bottom and extending offshore beyond the shoreline. Ahrens (1990) introduced the concept of critical mass, which is the mass of stones needed to maintain stability under a given wave condition. The experiment showed that while the gravel beach slope was dependent on wave conditions, there was almost no difference between equilibrium profiles formed from different initial beach profiles under same wave conditions. This was also observed by van der Meer & Pilarczyk (1986) through a similar laboratory experiment of a shingle beach for deep water wave conditions. This work suggests that it may not be necessary to precisely place the material forming dynamic revetment–type structures as long the required crest height is built and sufficient volume is provided.

## 3. Methodology

The complete experimental methodology for this study can be found in Blenkinsopp et al. (In review).

### 3.1. Experimental facility

The DynaRev experiment took place in the Großer Wellenkanal, GWK large wave flume, during August and September 2017. The flume is situated at the Forschungszentrum Kuste (FZK Coastal Research Centre), which is a joint institution between the University of Hanover and the Technical University Braunschweig located in Hanover, Germany. The flume is 309 m long, 7 m deep and 5 m wide and is equipped with a combined piston–flap–type wave paddle. Reflected waves and low frequency resonance (*e.g.* seiche) are damped at the paddle using an Automatic Reflection Compensation (ARC). A large–scale facility was necessary for this experiment due to the bimodal nature of the beach–revetment system. Scaling sediments to work in a smaller scale facility while retaining the particle diameter ratio of the cobbles and sand would result in cohesive sediment on the sand beach. It is noted that the 2D nature of this facility does not allow us to consider the influence of longshore sediment transport or short crested waves on the revetment performance.

The coordinate system is defined as follows: the vertical elevation, $z$ is defined positive upwards from the base of the flume; the cross–shore coordinate system, $x$ has its origin at the wave paddle and is positive in the direction of the beach. A sandy beach with an initial plane slope of 1:15 was installed on a permanent asphalt slope with a gradient of 1:6 located at the far end of the flume. The sand used to form the beach had the following characteristics: $D_{50} = 0.33$ mm, $D_{90} = 0.65$ mm and $D_{10} = 0.20$ mm. The beach was constructed to an elevation of 6.8 m above the flume bed. A 0.5 m thick layer of sand extending 25 m from the toe of the beach was placed to provide an additional store of sand seaward of the main beach slope (Figure 2). Therefore, the toe of the beach slope was located at $x = 188.5$ m and the top of the beach at $x = 283$ m. The total amount of sand required to build the beach was 1660 m$^3$.

### 3.2. Experimental set–up and instrumentation

A mechanical profiler was used to measure the beach profile after each run (see terminology in Section 3.3.1 and Section 3.3.2). It consists of a mechanical roller attached to an overhead mobile trolley running along the flume side walls. The system enables measurements of the complete bed profile to approximately $1 - 2$ cm vertical accuracy.

An array of three SICK LMS 511 Lidar scanners was used to measure the time–varying water surface elevation along an 80 m transect on the flume centreline. All three Lidars were sampled by a single computer at a scan rate of 25 Hz and angular resolution of 0.166 deg. Each Lidar is capable of obtaining measurements within a 190 degree field of view, though here we consider only the central 150 degrees within which valid water surface measurements were obtained. The Lidars were mounted in the flume roof at $z = 11.80$ m, (7.3 m above the initial still water line) at cross–shore locations $x = 230$ m, $x = 242$ m and $x = 255$ m and looked vertically down (Figure 2).

A high definition IP camera was mounted in the flume roof at $z = 11.8$ m and $x = 272$ m, and was facing the wave paddle. A series of ground control points (GCPs) were positioned within the camera field of view in order to rectify the generated timestack images of the swash zone. In combination with the most landward Lidar, the timestack images of swash flow can be used to infer the time–varying shoreline.

The movement of individual cobbles within the dynamic revetment was monitored using a Radio Frequency Identification (RFID) tracking system similar to that used by Allan et al. (2006). The RFID system consists of three components: Passive Integrated Transponder (PIT) tags, a module reader and a detection antenna. A total of 97 cobbles were fitted with transponders: 20 were painted in pink and placed on the bottom layer of the revetment (at the sand interface), from $x = 257.4$ m to $x = 259.8$ m; 30 were painted in orange and placed 20 cm above the bottom of the revetment (mid layer), from $x = 258.6$ m to $x = 262.2$ m; 47 were painted in green and placed at the toe and on the top layer of the revetment, from $x = 257$ m to $x = 262.6$ m. Cobbles placed in the middle layer started further landward than in the other layers, as the revetment has a triangular shape and becomes thick enough only around $x = 258.6$ m. They were all positioned along the centreline of the revetment in groups of 3 cobbles — except at the toe, where 7 cobbles where placed — at 40 cm intervals. As the wave flume is effectively 2 dimensional, the centreline was considered to be representative of the profile, and sediment transport assumed to be only cross–shore.

### 3.3. Experimental procedure

The main objective of the experiment was to quantify the performance of a dynamic revetment under varying wave and water level conditions. This was done by obtaining two comparable datasets of a sandy beach only (named
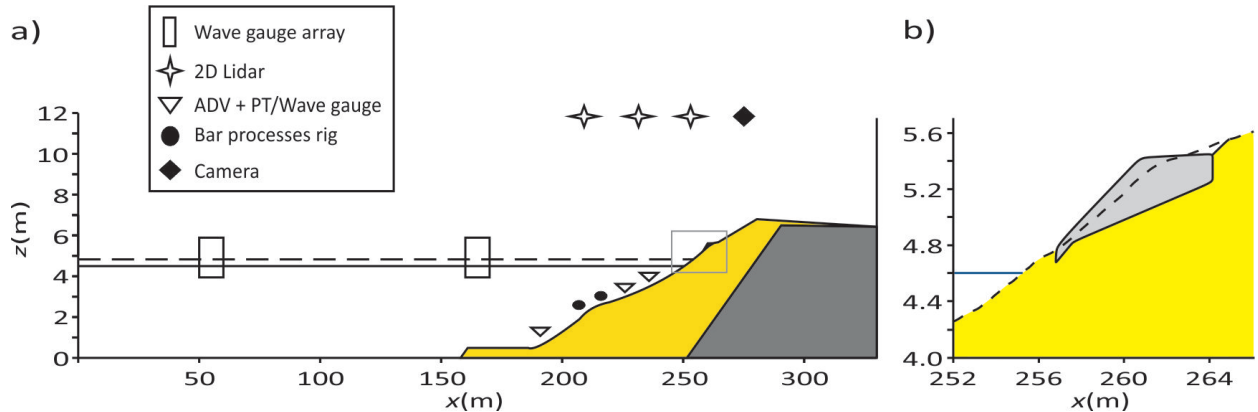
Figure 2: a) Schematic of flume setup showing primary instrument locations. The yellow shaded area represents the sand volume and the dark grey shaded area is the permanent 1:6 impermeable slope. The black solid and dashed horizontal lines indicate the minimum ($h = 4.5$ m) and maximum ($h = 4.9$ m) water levels. b) Close up of the dynamic revetment geometry after construction, corresponding to the grey box in (a). The light grey region indicates the dynamic revetment and the dashed line shows the beach profile prior to revetment construction.

phase SB) and a sandy beach protected by a dynamic revetment (named phase DR) under the same wave conditions and water level changes.

### 3.3.1. Phase SB: morphological response of a sandy beach

Run names for this phase are given as SB(E,A)<WL increment>—<Run No.>, where E and A stand for Erosion and Accretion respectively, water level (WL) increments are numbered 0 for the initial water level of $h = 4.5$ m to 4 for $h = 4.9$ m and run numbering is started from 1 for each WL increment. For example, SB1-2 corresponds to second run for the first water level rise for the Sandy Beach (SB) Phase. Runs had different durations, varying from 20 minutes up to 3 hours. Starting with a water level of 4.5 m, a standard wave case with a significant wave height $H_s = 0.8$ m (at the wave paddle), and a peak period $T_p = 6$ s was run for 20 hours. Time series of 2 hours of irregular waves were created from a JON-SWAP spectrum (using a peak enhancement coefficient of 3.3), and were repeated every 2 hours. This allowed the waves to reshape the beach profile to a developed beach profile approaching equilibrium (Table 1). The second part of Phase SB consisted of a series of 4 in-

cremental water level increases of 0.1 m using the standard wave conditions (Table 1). At the final water level, $z_{wl} = 4.9$ m, 2 erosive cases (labelled SBE) and 1 accretive case (labelled SBA) were run as part of a 'resilience test' (Table 1).

Table 1: Overview of the test programme for Phase SB: $H_s$ is the significant wave height at the wave paddle; $T_p$ is the peak period; $\Omega_0$ is the dimensionless fall velocity (also called Dean's number, $\Omega_0 = H_0/w_s T_p$, (Dean, 1973; Gourlay, 1968)) calculated using offshore significant wave height ($H_0$); and wave energy is given in MJ per metre of wave crest.

| Test | Dura-tion (hr) | $H_s$ (m) | $T_p$ (s) | Water level $z_{wl}$(m) | $\Omega_0$ | Ener-gy (MJ) |
|---|---|---|---|---|---|---|
| **Approach Equilibrium** | | | | | | |
| **SB0** | 20 | 0.8 | 6 | 4.5 | 3.38 | 0.78 |
| **Water Level Changes** | | | | | | |
| **SB1** | 7 | 0.8 | 6 | 4.6 | 3.38 | 0.78 |
| **SB2** | 7 | 0.8 | 6 | 4.7 | 3.38 | 0.78 |
| **SB3** | 7 | 0.8 | 6 | 4.8 | 3.38 | 0.78 |
| **SB4** | 17 | 0.8 | 6 | 4.9 | 3.38 | 0.78 |
| **Resilience test** | | | | | | |
| **SBE1** | 2 | 1 | 7 | 4.9 | 3.51 | 1.23 |
| **SBE2** | 4 | 1.2 | 8 | 4.9 | 3.54 | 1.76 |
| **SBA1** | 6 | 0.6 | 12 | 4.9 | 1.02 | 0.44 |

8

### 3.3.2. Phase DR: morphological response of a sandy beach with a dynamic cobble berm revetment

Run names for this phase are given as DR(E,R)<WL increment>—<Run No.>. For example, DR4-3 corresponds to third run for the last water level rise for the Dynamic Revetment (DR) Phase. Runs had different durations, varying from 20 minutes up to 3 hours. Before starting Phase DR, the beach was manually reshaped to the original 1:15 planar slope. Starting with a water level of $z_{wl} = 4.5$ m, the initial case of Phase SB was repeated with 20 hours of the standard wave conditions to obtain a developed beach profile approaching equilibrium that was almost identical to that at the end of SB0 (Table 2). Once the developed beach profile was reached, and before building the revetment, the beach was first flattened to 1:15 at the revetment location to ensure a sufficient volume of cobbles could physically be placed (see Blenkinsopp et al. (In review)). The revetment was placed by dumping stones and then reshaping to the required profile using a front–end loader and manual profiling. The dynamic revetment was constructed using rounded granite cobbles with the following characteristics (intermediate axis): $D_{max} = 90$ mm, $D_{min} = 50$ mm, $D_{50} = 63$ mm, $D_{85}/D_{15} = 1.32$ and a minor axis dimension of 30 mm on average. This well sorted material had a density of 2700 kg/$m^3$, and a bulk density of 1600 kg/$m^3$, giving a porosity of 0.41. Based on previous studies of slope steepness (e.g (Komar & Allan, 2010; van Hijum, 1976; Powell, 1988; Roman-Blanco et al., 2006)), the front slope of the revetment was set to 1:6.3, in agreement with the cobble characteristics (Powell, 1993). The toe of the revetment was located at $x = 256.8$ m, and $z = 4.77$ m, roughly corresponding to the predicted shoreline position for test DR3 ($z_{wl} = 4.8$ m). The predicted $R_{2\%}$ runup height for the standard wave condition was calculated as 0.72 m using the equation developed by Poate et al. (2016) for gravel beaches. Therefore, the crest was built at $z = 5.42$ m, putting the crest 0.65 m above the toe, at $x = 260.7$ m. This elevation corresponds to the predicted value of $R_2$ % for DR2 ($z_{wl} = 4.7$ m) and so consequently, it was expected that the revetment crest would be overtopped by approximately 2% of waves during testing at this water level increment. The crest of the revetment was horizontal until it intersected with the sand slope, at $x = 264.1$ m. Therefore, the total cross–shore length of the revetment was 7.3 m. The volume of the revetment was 9.375 m$^3$ with a total weight of 15 tonnes. Following construction of the revetment, the procedure used for tests SB1 to SB4 described in Section 3.3.1 was repeated, with the same water level elevations and run durations (Table 2).

The resilience test in Phase DR was modified from that used in Phase SB (Table 2) to investigate the relationship between the revetment front slope and wave period. A series of erosive tests with increasing wave energy were completed, followed by a two hour case using the standard wave condition, in order to observe the process of recovery after energetic conditions (Table 2).

Following the completion of the resilience testing, an extra 2.50 m$^3$ of material was added to the front slope of the revetment to increase the thickness of the revetment slope and crest width. The extra cobbles were placed with the same slope as the reshaped revetment (around 1:3.2) while retaining the same crest height. After renourishment of the revetment, a series of different wave cases were run to investigate the short–term response of the revetment front slope, at water level $z_{wl} = 4.9$ m Table 3.

### 3.4. Data Processing
#### 3.4.1. Volume of the revetment during the experiment

The thickness of the revetment was measured after each water level change test, after

Table 2: Overview of the test programme for Phase DR: $H_s$ is the significant wave height at the wave paddle; $T_p$ is the peak period; $\Omega_0$ is the dimensionless fall velocity (also called Dean's number, $\Omega_0 = H_0/w_sT_p$, (Dean, 1973; Gourlay, 1968)) calculated using offshore significant wave height ($H_0$); and wave energy is given in MJ per metre of wave crest.

| Test | Dura-tion (hr) | $H_s$ (m) | $T_p$ (s) | Water level $z_{wl}$(m) | $\Omega_0$ | Ener-gy (MJ) |
|---|---|---|---|---|---|---|
| Approach Equilibrium | | | | | | |
| DR0 | 20 | 0.8 | 6 | 4.5 | 3.38 | 0.78 |
| Construction of the dynamic revetment | | | | | | |
| Water Level Changes | | | | | | |
| DR1 | 7 | 0.8 | 6 | 4.6 | 3.38 | 0.78 |
| DR2 | 7 | 0.8 | 6 | 4.7 | 3.38 | 0.78 |
| DR3 | 7 | 0.8 | 6 | 4.8 | 3.38 | 0.78 |
| DR4 | 17 | 0.8 | 6 | 4.9 | 3.38 | 0.78 |
| Resilience test | | | | | | |
| DRE1 | 2 | 0.9 | 6 | 4.9 | 3.69 | 0.99 |
| DRE2 | 2 | 1 | 7 | 4.9 | 3.51 | 1.23 |
| DRE3 | 1 | 1 | 8 | 4.9 | 3.08 | 1.23 |
| DRR1 | 2 | 0.8 | 6 | 4.9 | 3.38 | 0.78 |

Table 3: Overview of the test programme for the recharged revetment testing at the maximum water level $z_{wl} = 4.9$ m: $H_s$ is the significant wave height at the wave paddle; $T_p$ is the peak period; $\Omega_0$ is the dimensionless fall velocity (also called Dean's number, $\Omega_0 = H_0/w_sT_p$, (Dean, 1973; Gourlay, 1968)) calculated using offshore significant wave height ($H_0$); and wave energy is given in MJ per metre of wave crest.

| Test | Dura-tion (hr) | $H_s$ (m) | $T_p$ (s) | Water level $z_{wl}$(m) | $\Omega_0$ | Ener-gy (MJ) |
|---|---|---|---|---|---|---|
| DRN1 | 2 | 0.8 | 6 | 4.9 | 3.38 | 0.78 |
| DRN2 | 0.66 | 1 | 8 | 4.9 | 3.08 | 1.23 |
| DRN3 | 2 | 0.8 | 6 | 4.9 | 3.38 | 0.78 |
| DRN4 | 0.66 | 1 | 9 | 4.9 | 2.73 | 1.23 |
| DRN5 | 0.33 | 1.2 | 8 | 4.9 | 3.54 | 1.76 |
| DRN6 | 1 | 0.8 | 6 | 4.9 | 3.38 | 0.78 |

the erosive tests and after the recovery test. Revetment thickness was established by digging a series holes in the revetment which could be refilled without damaging the initial revetment shape. This technique allowed the depth to the sand to be measured manually with a vertical accuracy of $1 - 2$ cm. Holes were dug approximately every 0.5 m cross–shore. The position of the toe and the back of the revetment were also surveyed during these measurements. A linear interpolation was used to obtain the interface between the revetment and the sand for the entire revetment width and this data combined with profiler measurements of the revetment surface were used to estimate the volume and shape of the revetment. At the end of the experiment, a channel was excavated along the centreline of the revetment to expose the sand–cobble interface and enable a complete profile to be measured. This enabled the revetment volume at the end of the experiment to be accurately determined and suggests that the technique described above is able to estimate revetment volume within 5 % (0.4 m$^3$) of the actual volume.

### 3.4.2. Swash detection

Timeseries of beach profile and swash surface elevation were obtained from the most landward Lidar, which was located directly above the exposed beach, using a method similar to that presented by Almeida et al. (2015). The raw lidar measurements capture the nearest surface, beach profile or swash surface, without any distinction between the two. To separate topography from the swash surface over time at each cross–shore position, the Lidar data was sub–sampled onto a 0.1 m horizontal grid and a moving–average window of 2 s with a mean variance threshold was applied to all measurements. This method of separating the stationary bed level (referred to here as the 'bed') from the non–stationary water surface (wave or swash, here referred to as the 'swash') is similar to that used by Turner et al. (2008) for data collected using ultrasonic bed-level sensors. Using this method, Lidar data were separated into timeseries of "swash" and "bed" elevation which can be analysed independently. Therefore, a timeseries of the shoreline position, defined by the location of the most landward "swash" position at every timestep, could be extracted. These runup data obtained from the Lidar were validated against visual *in situ* observations, and by plotting the shoreline timeseries on top of rectified

timestacks generated by the HD camera (Section 3.2).

### 3.4.3. Gross and net change rates

Using the "bed" timeseries extracted from the Lidar data it is possible to capture the exposed beach profile at high temporal resolution (25 Hz). From this dataset, a representation of the gross and net rates of change of the revetment volume were calculated.

Revetment profiles were extracted from the Lidar data every 6 seconds (approximately every wave) at a spatial resolution of 0.1 m. These data were used to calculate both the net and gross rate of absolute volume change per metre width between profiles by applying the trapezoidal rule and summing the absolute values.

Specifically, the rate of absolute volume change per metre width was calculated between each consecutive profile, and then averaged every 10 minutes to give an indicative rate of short–term volume change, ignoring the direction of change. The averaged value was finally divided by 6 to give the gross volume change (per metre width) per second, denoted $\overline{dV}$. Here, the gross rate of revetment volume change per metre width $\overline{dV}$ represents the rate at which the volume of the revetment is changing over short timescales.

In contrast, the rate of absolute volume change per metre width was calculated between profiles separated by 10 minutes, and then divided by this duration. This is hereafter named the net volume change (per metre width) per second, and is denoted $dV_{10}$. This value simply represents the mean rate of change over a 10 minute period.

## 4. Results

### 4.1. Revetment behavior

### 4.1.1. Comparison of Phase SB and DR

Figure 3 shows the overall evolution of the bed relative to the original planar profile. Bed elevation was extracted from the profiler and Lidar data, and bed changes relative to the initial planar profile were computed at every second throughout the experiment, for Phase SB (Figure 3a) and Phase DR (Figure 3b). Note that the revetment was built at $t = 0$ h on Figure 3b. This explains the sudden accretion between $x = 259$ m and $x = 262.5$ m showing the revetment installation, and the sudden erosion between $x = 262.2$ m and $x = 264.8$ m showing the sand compaction during cobble placement.

Bed evolution during the first 20 hours (from $t = -20$ h to $t = 0$ h) was almost identical for Phase SB (Figure 3a) and Phase DR (Figure 3b), suggesting that laboratory experiments investigating morphological change are repeatable at this scale. Differences in bed change can be observed between Phase SB and Phase DR once the revetment is installed, and particularly around the beachface. The shoreline and the berm (small sand berm in light blue around $R_{2\%}h$ on Figure 3a; cobble berm in light blue in Figure 3b) retreated further landward during Phase SB than Phase DR, leading to reduced horizontal runup excursions during Phase DR (Section 4.3 and Section 4.4). The presence of the revetment limited the erosion of the beachface during energetic conditions (runup data not available) and altered the evolution of the outer bar, which appears more stable during Phase DR than Phase SB.

These differences are also seen on Figure 3c which shows a series of profiles comparing the response of the beach with and without the revetment. It is clear that the profile at the start of SB1 and DR1 are very similar, with the exception of the revetment area. Over the course of the water level increments, the offshore bar in Phase DR tends to be a little higher, and later in the tests, further landward than in Phase SB. During the water level changes, the defined trough and inner bar evident landward of the outer bar at the start of the first water level increment (SB1, DR1) are smoothed out and become less pronounced.
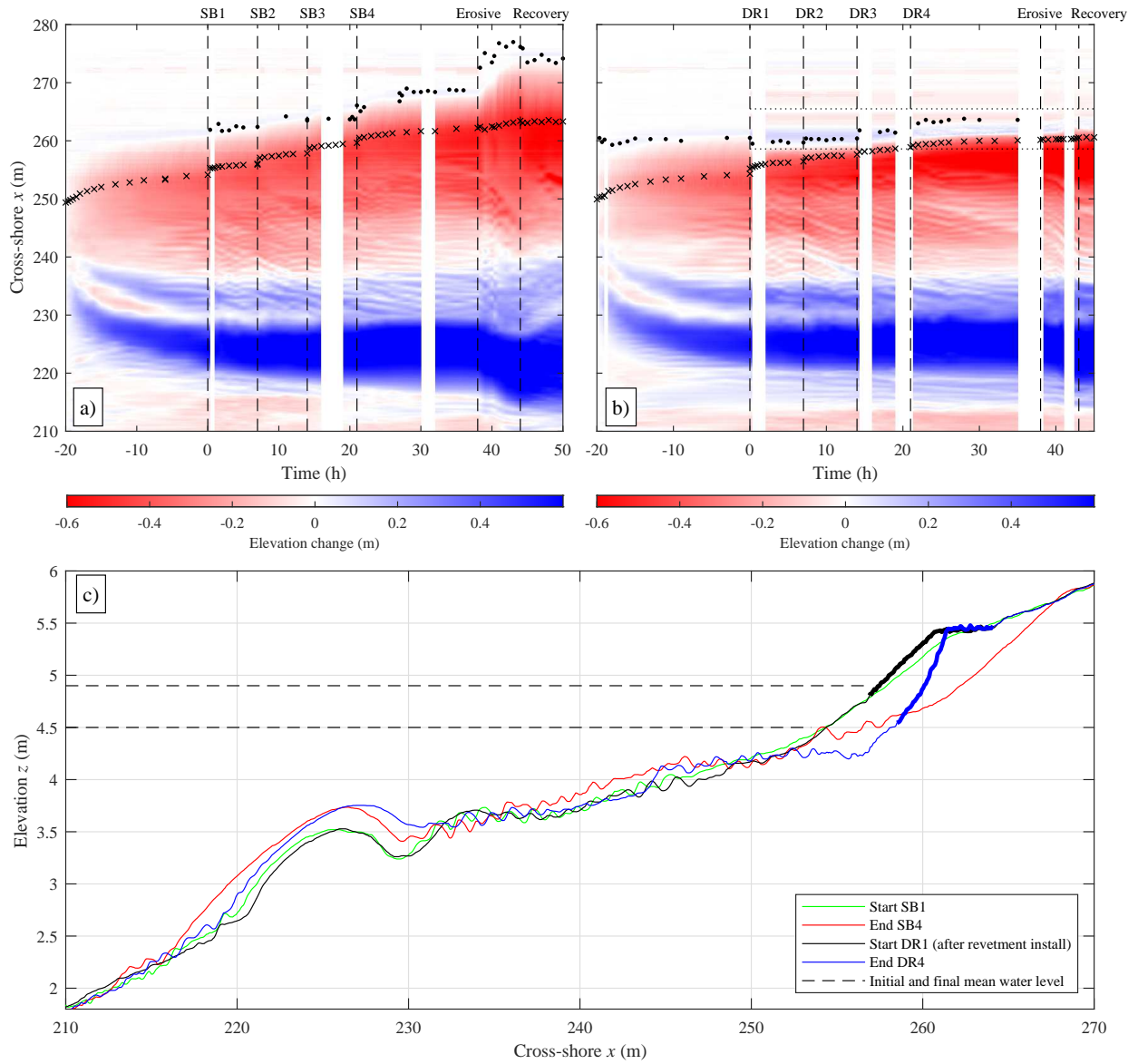
Figure 3: Bed elevation change relative to the original planar profile, for (a) Phase SB and (b) Phase DR. Red represents erosion and blue accretion. The vertical dashed lines mark the beginning of a new water level (*e.g.* DR1, DR2,...) and resilience test cases (*e.g.* erosive and accretive). The black dots represents $R_{2\%}h$, which is the horizontal runup limit exceeded by 2 % of the wave runup (note that data are not available for all runs). The black crosses represent the shoreline position, taken at the end of each run. The horizontal and parallel dotted lines on (b) mark the most seaward and landward limit of the revetment. (c) shows the beach profile at the beginning of SB1 (initial water level of 4.5 m) in green and DR1 in black; and at the end of SB4 (final water level of 4.9 m) in red and DR4 in blue. The revetment surface is marked with a thicker line.

Between the shoreline and the sandbar, sand ripples with a wavelength greater than one metre are evident in all profiles. During Phase SB, the bed elevation in this region rises by approximately 0.20 m as the water level increases by 0.4 m. This is not the case for the Phase DR testing, and the bed between the revetment toe and the bar remains at approximately the same elevation. At the end of testing, the main difference between the two tests is the erosion area directly adjacent to the revetment toe, as well as the ripple area in inner surf zone. In this region, profile DR4 is approximately 0.25 m lower than profile SB4 $x = 252$ m and $x = 258$ m. This local erosion may be influenced by the increase in wave reflection caused by the presence of the revetment in Phase DR. The coefficient of reflection at the end of SB0 and DR0 was around 0.200. At the end of the final water level increment, the coefficient of reflection decreased to 0.180 for SB4 whereas it increased to 0.225 for DR4.

Significant erosion of the sand beachface is observed during the Phase SB testing (Figure 3a and c). The shoreline retreated (due to both water level rise and sand loss) by 12.8 m over the course of the water level increments, and erosion was observed up to $x = 268$ m. The presence of the revetment slowed this retreat considerably, with the shoreline retreating by approximately 9.7 m (Figure 3b and c). Over the course of the water level increases, the revetment crest elevation was relatively stable but it retreated by 0.9 m overall. Additionally, the toe of the revetment retreated by approximately 1.7 m and lowered by 0.28 m. This led to an overall steepening of the revetment from 1:6.3 to 1:2.3. Although the crest of the cobble structure was overtopped completely by multiple waves, the horizontal runup extent was greatly reduced when compared to the SB cases (Section 4.3), and no beach change is observable in the profile measurements landward of the back of the revetment at $x = 265$ m.

### 4.1.2. Evolution of the revetment

During DR1 ($z_{wl} = 4.6$ m) and DR2 ($z_{wl} = 4.7$ m), the original crest was not overtopped (Figure 6). The maximum $R_{2\%}$ limit is shown by a blue dot in Figure 4b and Figure 4c, and it is observed that a small intermediate berm was created just below this elevation. The majority of morphological change occurred around the toe and lower part of the front slope of the revetment (below the intermediate berm), causing steepening in this region. At the end of DR2, the toe of the primary revetment volume is located 7 cm lower than the original elevation, at $z = 4.69$ m (Figure 5a), and has moved 0.9 m landward (Figure 5b). In addition, a mixed layer of cobbles and sand was formed at the toe (shown in green on Figure 4a and Figure 4b), and extends to the original toe position at $x = 256.8$ m. Globally, the crest and the centroid remain stable in elevation and horizontal position (Figure 5a, Figure 5b), although the landward movement of the toe brings the centroid slightly landward by 16 cm. This caused the revetment to shorten by 0.7 m in cross–shore extent (Figure 5c), and increase in height from 0.65 m to 0.76 m (Figure 5c).

At the end of DR3 ($z_{wl} = 4.8$ m), after 7 hours of waves (Figure 4d), the original crest started to be overtopped by around 10 % of wave runup events (Figure 6). The maximum $R_{2\%}$ limit is now landward the crest, at $x = 261.6$ m (Figure 4d). A lot of water percolated through the structure during the overtopping events, which transported sand seaward from beneath the revetment and caused the front slope to steepen further. This steepening again occured primarily in the lower and mid swash, although the intermediate berm observed previously is now indistinct. The region of sparse cobbles and sand lengthened (Figure 4d). As shown in Figure 5b, the revetment crest, centroid and toe retreated by 0.4 m, 0.3 m and 0.9 m respectively. Therefore, the cross–shore length of the revetment decreased to 5.6 m.
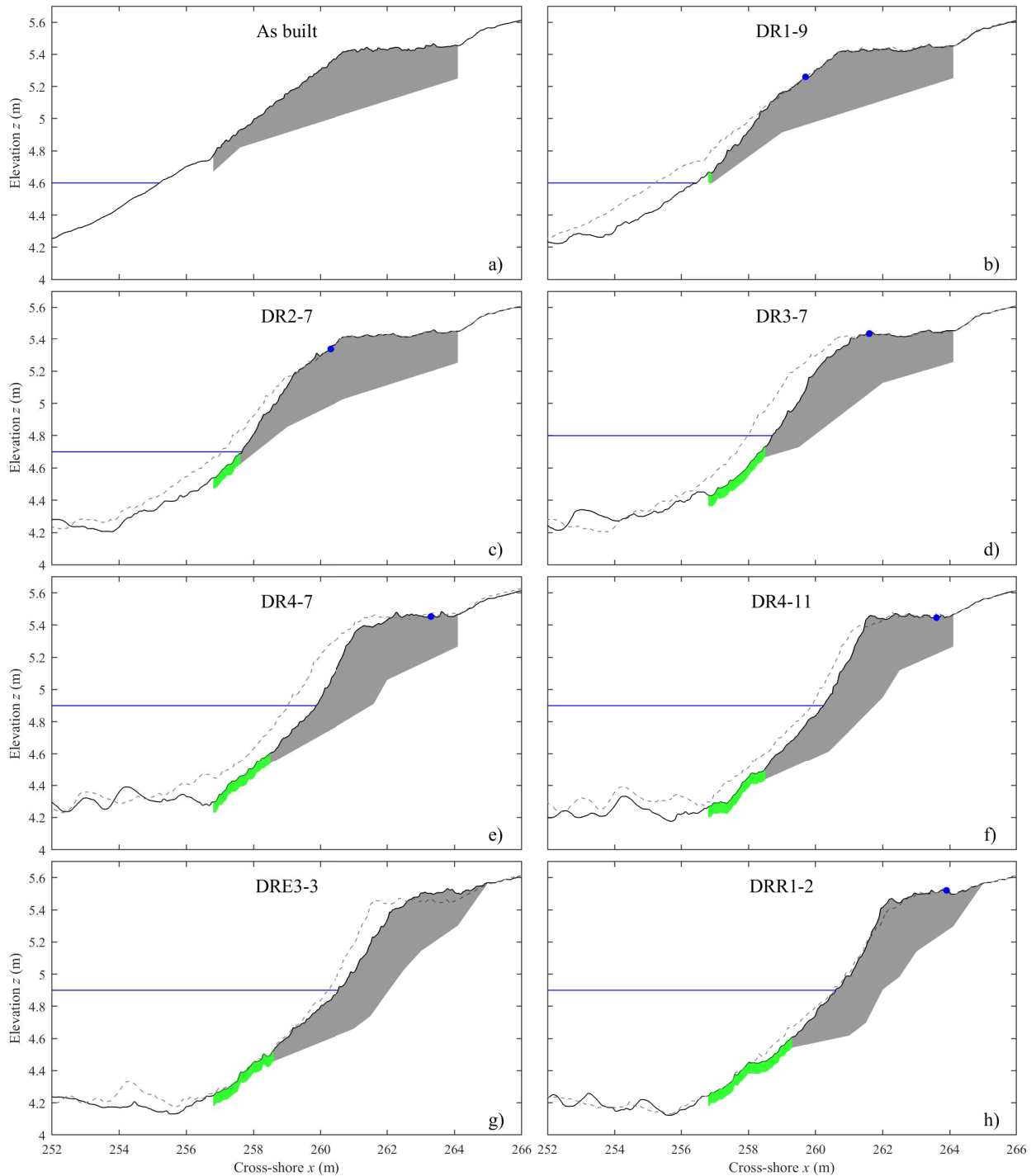
Figure 4: Shape of the dynamic cobble berm revetment, showing: (a) revetment shape as built, DR1-0; (b) revetment shape after 7 hours of testing at $z_{wl} = 4.6$ m water level, DR1-9; (c) revetment shape after 7 hours of testing at $z_{wl} = 4.7$ m water level, DR2-7; (d) revetment shape after 7 hours of testing at $z_{wl} = 4.8$ m water level, DR3-7; (e) revetment shape after 7 hours of testing at $z_{wl} = 4.9$ m water level, DR4-7; (f) revetment shape after 17 hours of testing at $z_{wl} = 4.9$ m water level, DR4-11; (g) revetment shape after the 2 erosive cases of the resilience test, DRE3-3 (5 hours); (h) revetment shape after the recovery case of the resilience test, DRR1–2 (2 hours). The grey areas represent the part of the revetment composed of cobble only (no mixing with sand). The green layer areas represent a single layer of cobble mixed with sand. The boundary between the grey and green shading corresponds to the toe of the primary revetment volume. The blue dot represents the maximum cross–shore position exceeded by 2 % of wave runup. The dashed line shows the surface of the revetment as on the previous panel.

14

The revetment was observed to sink slightly due to the sand erosion occurring underneath, so the crest and centroid elevation decreased by 1 cm and 2 cm respectively (Figure 5a). The total revetment height fluctuated between 0.65 m and 0.74 m during DR3 (Figure 5c). This was mainly driven by the variation of the toe elevation (Figure 5a).

As soon as the water level was raised to $z_{wl} =$ 4.9 m (DR4), the percentage of overtopping increased significantly, up to 65 % (Figure 6) and the maximum $R_{2\%}$ limit moved further landward. This caused steepening over the entire front slope of the revetment which seemed to approach an equilibrium with a value of 1:2.3 at the end of DR4 (Figure 4f). Toward this equilibrium, the crest, toe and centroid positions retreated (Figure 5b). The elevation of the toe and centroid dropped while the elevation of the crest increased (Figure 5a). As mentioned before, this lowering is due to the sinking process caused by the sand erosion occurring underneath the structure as the backwash percolates through it. In the meantime, it was observed that cobbles were being pushed over the crest, rolling upward and landward through rollover transport (demonstrated in Section 4.2). It is suggested that this rollover transport counter–acts the sinking process, maintaining the crest at an almost constant elevation with a little gain in elevation at the end of DR4 (Figure 5az. Without this rollover transport it is hypothesised that the structure crest would be much lower. It is unclear at present what are the main drivers of this sand erosion. Nonetheless, this sinking process needs to be considerate for revetment design and will be further discussed in Section 5. Overall, sand erosion and rollover transport led to an increase in total revetment height from 0.68 m to 0.95 m, and a stabilisation of the revetment length around 5.6 m (Figure 5c).

After 38 hours, a series of erosive tests with increasing wave energy were completed as part of the resilience testing, followed by a two hour
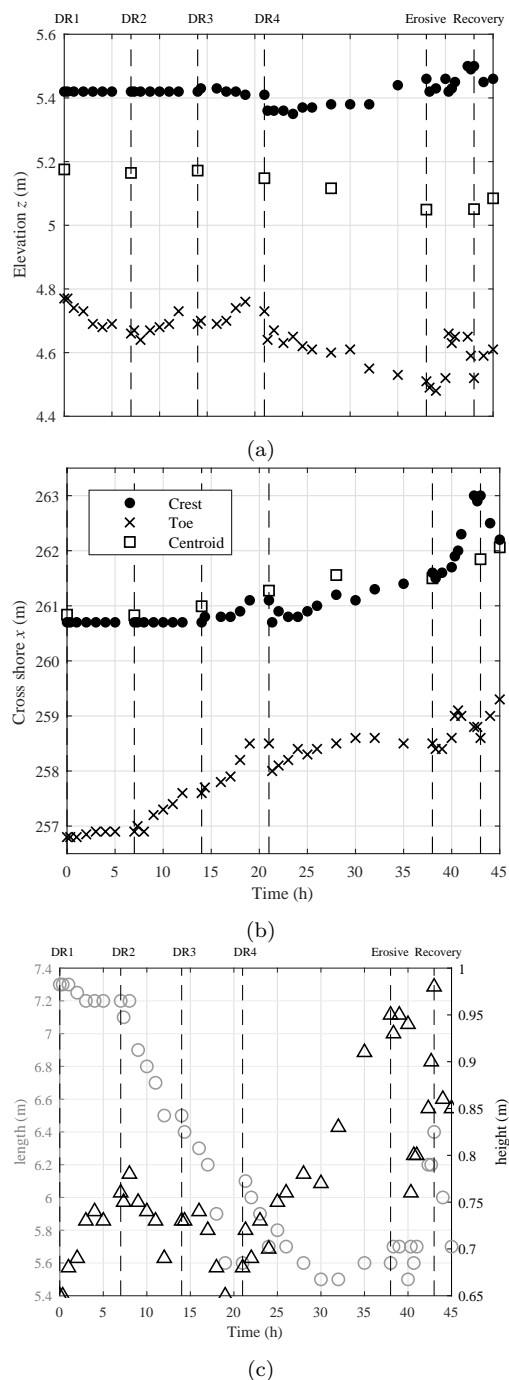


Figure 5: (a) Vertical, and (b) horizontal evolution of the crest, toe and centre of gravity of the revetment through time. The crest (dots) height is defined as the averaged elevation of the flat area at the top of the revetment. The toe (cross) is defined as the toe of the cobble body, corresponding to the toe of the grey area on Figure 4. The centroid (square) is defined as the centre of mass of the cobble body. Each cross and dot corresponds to a run. The squares correspond to the end of the runs showed in (Figure 4). (c) Evolution of the cross–shore extent (length) and height of the revetment through time. Each grey circle (length) and black square (height) corresponds to a run.The dashed lines marks the beginning of a new water level (*e.g.* DR1, DR2,...) and resilience test cases (*e.g.* erosive and recovery).

15

case using the standard wave condition (Table 2). At the end of DRE3 ($z_{wl} = 4.9$ m), increased runup was measured along with more frequent overtopping which spread the cobbles beyond the original landward limit of the revetment through rollover transport. This process flattened the revetment to a 1:3.15 slope and caused the overall length to increase to 6.4 m (Figure 4g;Figure 5c). It was observed (see Section 4.2) that cobbles from the toe were pushed onto the crest and beyond, thus the single cobble layer lengthened (Figure 4g). The crest, centroid and toe of the revetment retreated by 1.40 m, 0.10 m and 0.35 m respectively (Figure 5b). The crest became higher by 4 cm, whereas the centroid remained at the same elevation (Figure 5a). The toe elevation was highly variable, but ended at the same position as at the end of DR4, at $z = 5.52$ m. Overall, the height of the revetment increased to 0.98 m respectively, but was variable ($\pm 10$ cm) throughout the runs.

The recovery test (DRR) was observed to reshape the structure to its previous shape and slope of 1:2.3 (Figure 4h). The maximum $R_{2\%}$ limit was located slightly further inland than at the end of DR4, at $x = 263.9$ m (Figure 4f). A lot of material was brought upward from the toe during the previous energetic conditions, making it available for rollover transport. As a result, both the toe and the centroid increased in elevation to their final position at $z = 4.61$ m and $z = 5.08$ m respectively (Figure 5a). They also both retreated, by 0.20 m for the centroid and 0.7 m for the toe (Figure 5a). The crest location ended up slightly lower and more seaward than its previous position. This is mainly due to the method of measuring its position, which averaged the elevation of the flat area at the top of the revetment. Figure 5. The revetment is back to what seems to be its equilibrium length of 5.7 m, for a height of 0.85 m (Figure 5c).
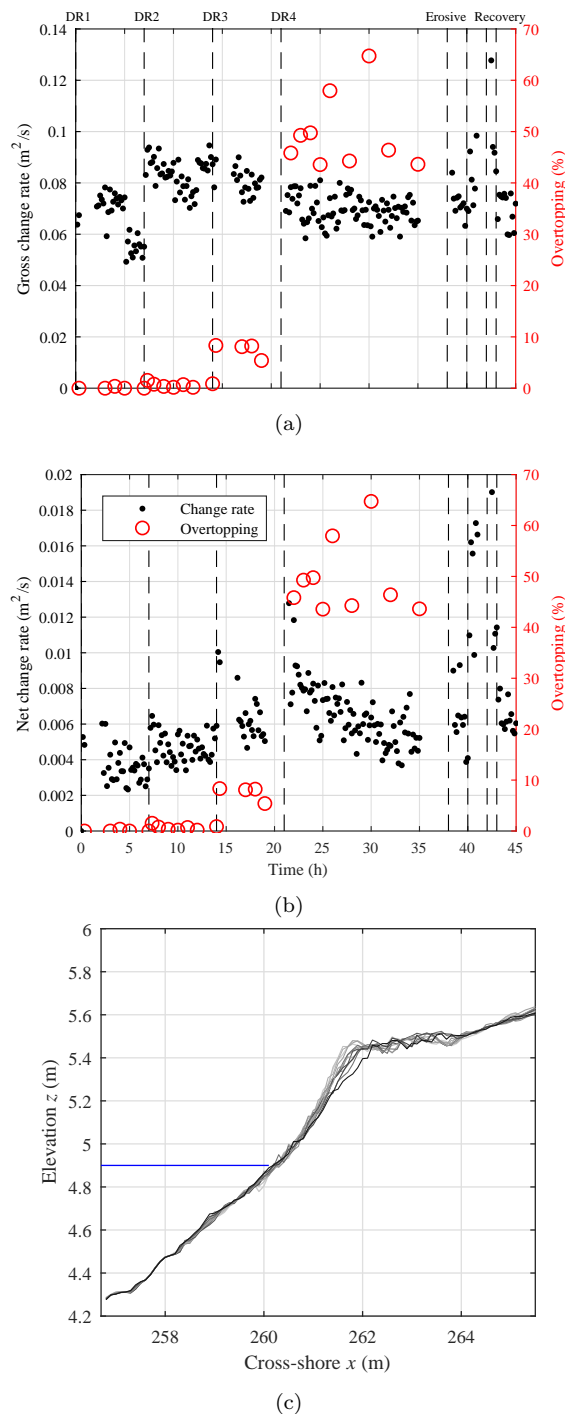
16



(a)

(b)

(c)

Figure 6: *Left axis*: (a) Gross rate of volume change per second $\overline{dV}$ (black dots): The change of revetment volume per metre width was calculated every 6 seconds (so roughly every wave), as the sum of the absolute difference between consecutive profiles. An average value was then calculated every 10 minutes to give the average per second volume change over this period. The percentage of overtopping is shown by the red circles. (b) Net rate of volume change per second $dV_{10}$ (black dots): The change of revetment volume per metre width was also calculated every 10 minutes, as the sum of the absolute difference between 2 bed profiles. A mean rate of change per second over the whole 10 minute period was then calculated. The dashed lines marks the beginning of a new water level (*e.g.* DR1, DR2,...) and resilience test cases (*e.g.* DRE1, DRR1,...). The percentage of overtopping is shown by the red circles. (c) Profile of the revetment plotted each 5 minutes for DRE2 (1h test). Light grey corresponds to the beginning of the run, and dark the end.

### 4.1.3. Revetment stability

The global changes in revetment profile observed in the previous section are the integrated result of smaller and rapid changes in beach profile. This can be observed and measured by the Lidar on a wave by wave basis. As described in Section 3.4.3, the gross rate of volume change, $\overline{dV}$ and the net rate of volume change, $dV_{10}$ were calculated over the revetment area using the Lidar data. It is important to note that these estimates include the elevation changes due to sand erosion occurring underneath the structure.

Figure 6a and Figure 6b indicate that overtopping started to occur during test DR3 ($z_{wl} = 4.8$ m) but rates remained smaller than 10 %. A sudden increase to around 50 % of waves overtopping the structure crest was observed during DR4 when the water level was raised to $z_{wl} = 4.9$ m.

The net rate, $dV_{10}$ was observed to increase with each water level increment as more of the revetment was exposed to swash flows (Figure 6b). During DR4, although overtopping remained around 50 %, the net rate was observed to decrease approximately linearly to around 0.005 m$^2/s$. It is suggested that this is evidence that the revetment is approaching an equilibrium and this will be discussed further in Section 5. During the erosive runs of the resilience testing, the net rate increased, however when the standard wave case was used again in run DRR1, a net rate of 0.005 m$^2/s$ was measured in agreement with that at the end of DR4.

The gross rate of change throughout runs DR1 to DR4 are relatively stable at approximately 0.07 m$^2/s$, with small changes occurring with each water level increment as the position of the swash zone changes (Figure 6a). During the energetic runs of the resilience testing (DRE1, DRE2, DRE3) higher rates of gross change are measured. However when the wave energy is reduced again to the standard test case (DRR1), the gross change rate returns to
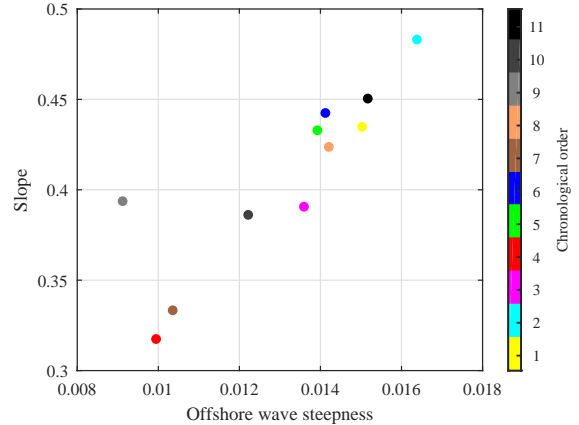


Figure 7: Revetment face slope as a function of the offshore wave steepness. The colours represent the chronological order of the observed slopes.

approximately 0.07 m$^2/s$ suggesting that this gross rate of change is primarily dependent on the wave energy. This is supported by the fact that there appears to be no effect of the high rates of overtopping during DR4 on the measured gross rates of volume change.

Figure 6 indicates that the gross rate of volume change is an order of magnitude larger than the net rate. This suggests that the revetment surface is highly dynamic, moving significantly with every wave, while the overall shape of the revetment remain stable.

During the resilience testing it is noticeable that the revetment shape (including the front slope and crest position) responds rapidly to changes in wave conditions. Figure 6c shows the profile of the revetment every 5 minutes during test DRE2 where it is observed that the top of the slope flattens, leading to a landward migration of the crest over just 1 hour. A clear relationship was identified between the revetment face gradient and the offshore incident wave steepness (Figure 7), with the slope increasing with offshore incident wave steepness. This was not influenced by the previous state of the revetment and suggests that an equilibrium revetment slope exists for a given wave condition, at least for this type of material.
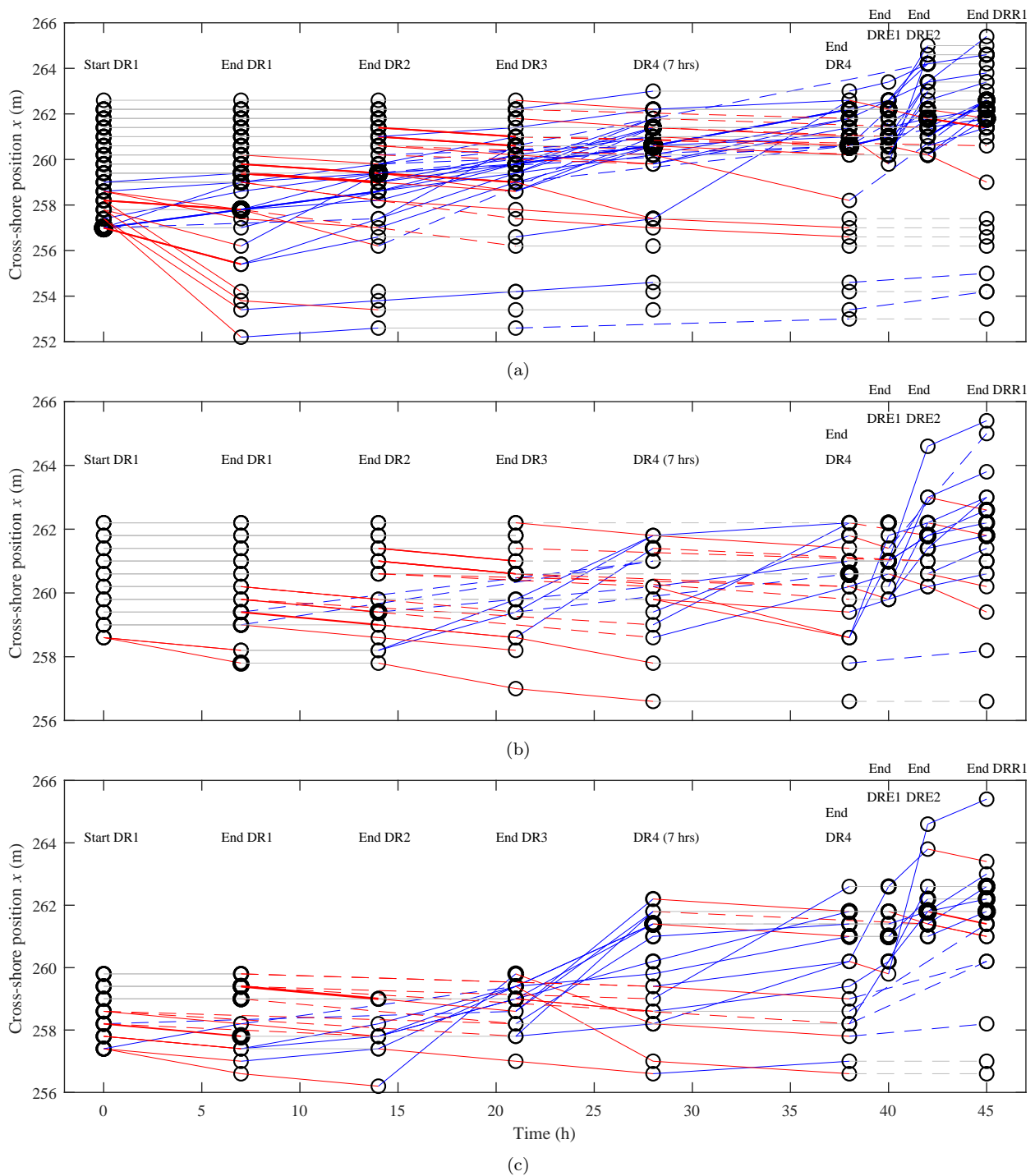
17

Figure 8: Cross shore position of the 97 tagged cobbles as a function of time, and for the three different layers (Section 3.2): (a) top layer; (b) middle layer; and (c) bottom layer (sand–gravel interface). The position of the cobbles was measured to the nearest 0.4 m in the cross–shore direction at the end of every water level increment and after each resilience test (except DRE3). The black circles represent the instrumented cobbles at each 0.4 m cross–shore increment and the thickness of the circle is relative to the number of cobbles at each location. Plain red lines correspond to seaward transport. Plain blue lines correspond to landward transport. Plain grey lines correspond to no transport. The thickness of the lines is relative to the number of cobbles moving along a particular path. The dashed lines indicate that a cobble was not detected for at least one detection survey, but was found again later. The same colour and thickness principles apply for the dashed lines.

18

## 4.2. Cobble tracking

Instrumented cobbles were initially placed along the centreline of the flume, at different elevation within the revetment (layers, see Section 3.2) and in groups of 3 — except at the toe where 7 cobbles were placed. This initial setup can be seen in Figure 8, and corresponds to the circle at $t = 0$ ('Start DR1'). The position of the instrumented cobbles was then measured after each change in water level or wave conditions (Figure 8). Note that the cobbles in the top and bottom layers extended to the initial revetment toe, however the first group of cobbles in the middle layer was 1.2m landward of the toe. Additionally the cobbles in the middle and top layers extended further landward than the bottom layer

Figure 8a shows that 4 of the cobbles initially placed around the toe ($x = 257$ m to $x = 258.2$ m) moved offshore between $x = 252.8$ m and $x = 255$ m over the course of the experiment and did not return to the revetment structure. These cobbles were lost offshore primarily during DR1 and account for 4 % of the total number of instrumented cobbles. Figure 8a also indicates a second group of cobbles between $x = 256.2$ m and $x = 257.4$ m, which were moved offshore of the initial toe during the experiment and formed the single layer of mixed sand and cobbles discussed in Section 4.1.2 (see green region in Figure 4). Of these cobbles some remained in this region for the remainder of the experiment, while some were subsequently transported landwards back onto the main revetment structure. This single layer area is also visible in Figure 8b and Figure 8c.

Figure 8 shows that landward cobble transport was often characterised by large cross–shore 'jumps' whereas seaward cobble transport is characterised by more progressive movements. There is also evidence that once cobbles were transported over the crest, they tended to remain there causing cobbles, particularly those initially in the top layer, to collect on the

crest over the course of the experiment. Figure 8 also shows that this rollover transport was intensified with wave energy, with the energetic runs of the resilience test mainly causing landward transport. While cobble movement is most evident in the top layer as expected, all cobbles in the mid and bottom layers were mobilised over the course of the experiment as they became directly exposed to swash once cobbles previously present on their seaward side were transported landward. Figure 8 indicates that most cobbles in all layers were initially transported seaward a short distance, before moving landward. A possible reason for this is that cobbles initially rolled seaward down the revetment slope under gravity before being pushed landward by wave runup. As a result, the overall transport motion appeared to be dominated by landward transport.

Overall, at the end of DR4, 74 (76.3 %) cobbles were detected and of these, 42 (56.7 %) cobbles had moved landward (upward), 28 (37.8 %) had moved seaward (downward) from their original position and 4 (5.5 %) cobbles remained at their original locations. A total of 23 cobbles (23.7 %) were not detected: they could have been deeply buried within the structure, or the their signal might have interfered with another one, or they could have simply been missed during the survey.

At the end of the resilience tests, 81 (83.5 %) cobbles were detected and of these, 59 (72.8 %) cobbles had moved landward (upward) and 19 (23.5 %) had moved seaward (downward) from their original position and 3 (3.7 %) cobbles had remained at their original locations. A total of 16 (16.5 %) cobbles were not detected.

## 4.3. Wave Runup

Figure 9 shows a comparison of the measured 2 % exceedance vertical ($R_{2\%}v$) and horizontal ($R_{2\%}h$) runup limits for each run and water level during phase SB and DR (the value is given with respect to the used water level). The presence of the revetment reduced the vertical runup by 17 %, 20 %, 27 % and 39 % for

DR1, DR2, DR3 and DR4 respectively (Figure 9a). It is evident that for Phase SB, there is a direct relationship between $R_{2\%}v$ and the horizontal runup extent — *i.e.* as the water level rises, the vertical ($R_{2\%}v$) and horizontal ($R_{2\%}h$) runup increase. This is not the case for Phase DR because the flat revetment crest leads to a physical limit for the runup height ($R_{2\%}v$) but has a smaller influence on horizontal excursion ($R_{2\%}h$). This is particularly noticeable during DR4 when there is a reduction in $R_{2\%}v$ but the horizontal excursion continues to increase. Comparing Phases SB and DR, the presence of the revetment reduced the horizontal runup by 2.4 m, 3.3 m, 4.3 m and 4.9 m for DR1, DR2, DR3 and DR4 respectively. It seems that the horizontal runup is minimised when the interaction between swash, cobbles and interstices is maximised, as is the case during DR4. In addition, the coefficient of reflection is at its maximum during DR4 and at its minimum during SB4. Therefore, the total energy reaching the beach is smaller for DR4 than SB4, and this can explain the trend of runup differences between the 2 phases.

## 4.4. Shoreline retreat

Figure 10 shows the evolution of the horizontal position of: (1) the intersection between the water level and sand beach during Phase SB, (2) the intersection between the water level and revetment surface during Phase DR, (3) the intersection between the water level and sand interface beneath the revetment during Phase DR (Figure 10a; (4) the berm, taken as the highest point on the beachface (Figure 10b). The locations of these interfaces are shown at the end of each water level increment and after the beach has received the same amount of energy from waves within the resilience test (the resilience test being different for each phase). For both the measured shoreline and sand interface underneath the structure, the presence of the revetment slowed down their retreat under wave action.
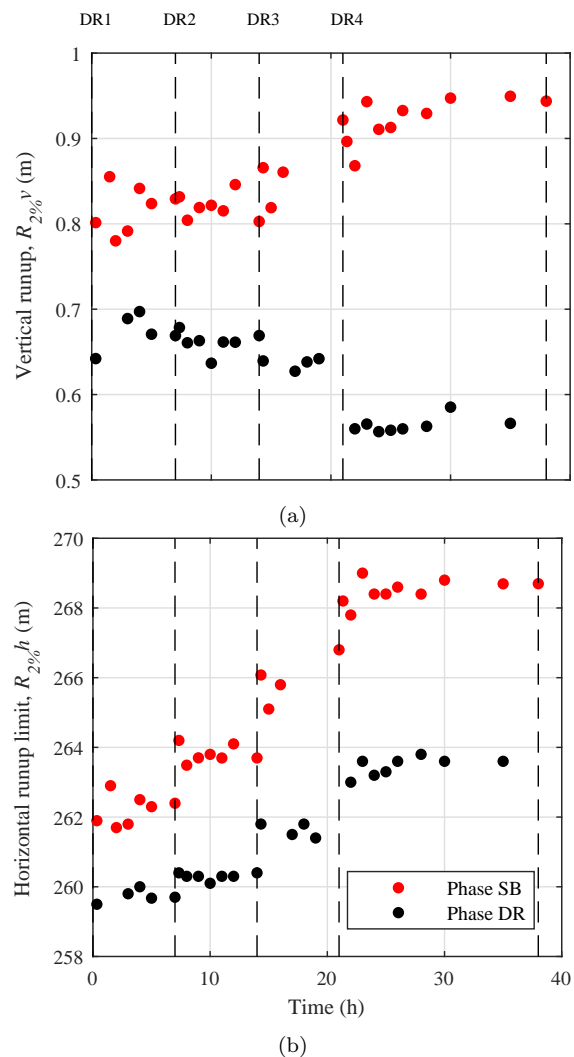


Figure 9: Comparison of (a) the $R_{2\%}v$ vertical runup height and (b) $R_{2\%}h$ horizontal runup limit for Phase SB (red dots) and Phase DR (black dots). Note that values from the resilience tests are not shown. The dashed lines marks the beginning of a new water level (*e.g.* DR1, DR2,...).
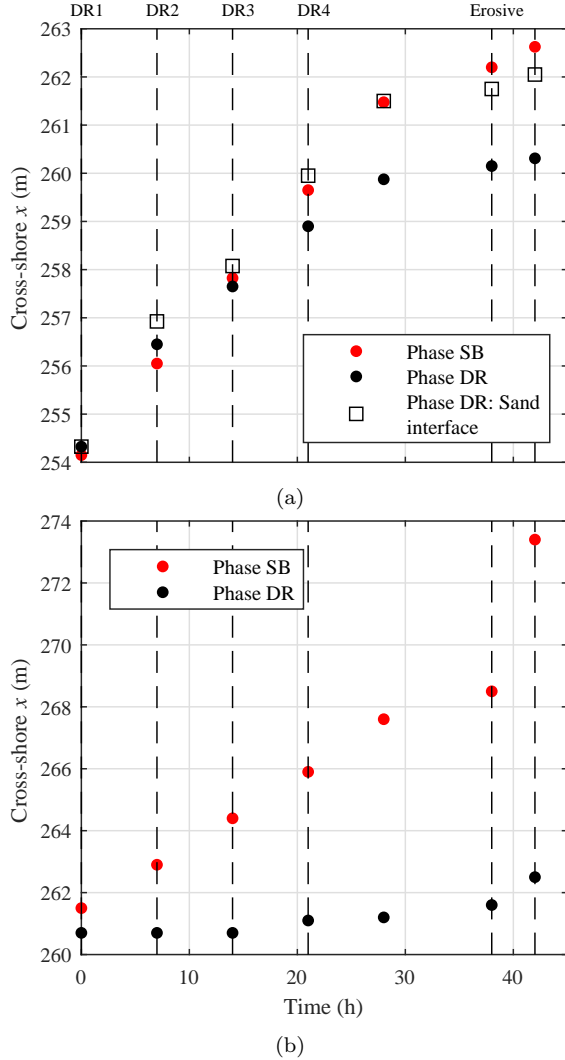
Figure 10: a) Comparison of the evolution of the horizontal position of: *red circle*: the intersection between the water level and sand beach during Phase SB; *black circle*: the intersection between the water level and revetment surface during Phase DR; *black square* the intersection between the water level and sand interface beneath the revetment during Phase DR. The sand interface under the revetment is obtained from *in-situ* measurements which were interpolated to estimate the position of the sand surface. The dashed lines marks the beginning of a new water level (*e.g.* DR1, DR2,...) or resilience test case (*e.g.* erosive). b) Comparison of the evolution of the berm position during Phase SB (red dots) and Phase DR (black dots).

For Phase DR, the sand interface under the revetment was interpolated from *in-situ* measurements, and the estimated sand shoreline is presented in Figure 10a. The sand depletion at the beginning of DR1, corresponding to the manual adjustment of the slope before the construction of the revetment, is evident (see Section 3.3.2). Despite this lack of sand at the beginning of the revetment testing, the sand interface retreated more slowly during Phase DR than during Phase SB. Indeed, even though the sand interface at the start of DR1 starts 0.8 m landward of that at the beginning of SB1, the final position shown in Figure 10a is 0.5 m further seaward for Phase DR. The ratio of the volume of sand on the sub–aerial beach for Phase DR to that for Phase SB is 1.0673 at the end of DR4/SB4, and 1.0964 at the final position shown in Figure 10a, meaning that there is respectively 6.73 % and 9.64 % more sand on the sub–aerial beach when the revetment is present. Similarly, the berm position moved further landward during Phase SB than Phase DR (Figure 10b). The revetment limited the total berm retreat to 2 m while the unprotected beach experienced a total retreat of about 10 m. The smaller berm retreat observed during Phase DR is a primary reason for the significant reduction in horizontal runup excursion discussed above.

## 5. Discussion

As with all flume experiments, the 2D nature of this experiment brings some limitations. Longshore sediment transport, short crested waves and oblique waves could not be tested, and therefore their impact on the processes presented in the results could not be explored. Longshore sediment transport, which is present on most coastlines, is expected to have an impact on cobble movement and the long–term resilience of dynamic revetments. However, at most locations it is expected that cross–shore processes will

most strongly influence the revetment evolution during storms, as welll as the sediment transport at the sand–cobble interface. It is suggested that future work should investigate the effect of longshore processes on composite beaches and dynamic revetments in the field. In particular, longshore transport of cobbles should be considered when designing dynamic cobble berm revetments for coastal protection and a replenishment programme would likely be required to maintain structure volume over time. The rate of replenishment can potentially be estimated by using one of the longshore transport equations developed for gravel (Kamphuis, 1991; CERC, 1984; Wellen et al., 2000; McCarroll et al., 2019) or for sand, gravel and shingle (Tomasicchio et al., 2013, 2015; van Rijn, 2014). Furthermore, it is suggested that future efforts focus on the development of a numerical model for composite beach and dynamic revetment. An initial investigation into modelling composite beach behaviour using the XBeach–G gravel beach model is presented by McCall et al. (2019), which highlighted the importance of accurately representing the sand erosion happening within the cobble berm to obtain robust predictions.

Figure 4 showed the global behavior of the dynamic cobble berm revetment as a coherent structure. The core body of the revetment represented in grey is always composed of at least 87 % of its original volume. Therefore, the retreat of the crest, toe and centroid of the revetment shown in Section 4.1.2 represents the retreat of almost the whole structure. This retreat was driven by two main processes:

1. the erosion of sand underneath the structure caused by water percolating through the cobbles and transporting sand seaward during swash backwash. This process caused the revetment to sink and steepen.
2. the rollover transport: RFID demon-

strated that 70 % of the instrumented cobbles ended up landward of their original position by the end of the resilience testing, and a large number of these were transported onto the revetment crest.

While rollover transport is a well–known phenomena for gravel beaches and berms (Lorang, 1991; Allan et al., 2006; Almeida et al., 2015), the sand erosion phenomena occurring underneath the cobbles has not been observed during monitoring of previously installed cobble berm revetments in the USA (Downie & Saaltink, 1983; Lorang, 1991; Allan et al., 2016, 2006; Komar & Allan, 2010; Allan & Gabel, 2016) and it is not an obvious feature on composite beaches. However, the lack of long term monitoring or field experiments on existing dynamic revetments and composite beaches partly explains the absence of information regarding this process. It is important to note that existing monitoring has only focused on surface changes and volume losses, with no measurements of the sand–cobble interface beneath the cobbles. However, van Gent (2010) undertook a laboratory experiment investigating the behaviour of a beach profile consisting of sand overlain by a uniform layer of gravel (porosity = 0.4) which extended the full length of the profile (test series S1). A profile shape similar to that observed during DR4 developed with an accretive berm and erosion below the SWL. However, no observations of the evolution of the sand–gravel interface were reported and it is possible that sand erosion underneath the gravel may have contributed to the observed erosion around the SWL.

Under water level increases, the sandy beach during Phase SB eroded as it evolved toward a new equilibrium (Figure 3c). A similar process appears to be happening to the sand underneath the revetment in Phase DR (Figure 4), with the sand profile beneath the revetment evolving in a similar manner to

the sand beach in Phase SB but at a slower rate. Note that in the present experiment, in order to get significant interaction between waves and cobbles, the revetment was placed at the location of the natural sand berm developed during DR0. Therefore, it was placed in an area which is prone to erosion as the water level is increased. As a result, the erosion demand occurring between $x = 255$ m and $x = 266$ m was at the location of the revetment. Similar sand erosion, as well as accretion, may occur in the field under changing hydrodynamic conditions. Future field work is required to understand how the combination of sand dynamics and rollover transport drives the overall change of a cobble berm over time.

As it retreated, the revetment remained a coherent structure with the majority of the individual cobbles remaining within the primary structure. Thus, despite being composed of relatively small cobbles which moved with every wave, the overall shape of the revetment structure was retained at all times during testing and the structure is considered dynamically stable. At the end of the resilience testing, the main body of the revetment retained 90 % of its original volume. In addition, the single mixed layer of sand and cobbles, represented in green on Figure 4, increased through the experiment and at the end of the resilience test, this layer accounted for a further 9 % of the original volume. As the revetment retreated, this layer remained attached to the structure, and is directly available to form part of the revetment under accretive conditions. Nevertheless, it is conservative to assume that this material is not part of the active protection anymore. The remaining 1 % is considered as lost offshore. Thus the results from the current experiment suggest that assuming at least 10 % loss of cobble volume from the main structure due to cross–shore processes is advisable. Of course

further, temporary cross–shore loss of cobbles following large energy events may also occur but this has not been observed in the current testing, even under energetic waves with large overtopping rates.

The observed dynamic stability of the revetment was also illustrated in Figure 6 where it was observed that the gross rate of volume change (per metre width), $\overline{dV}$ was 10 times bigger than the net rate $dV_{10}$. The relatively large gross rate of change suggests that there was significant cobble movement on a wave–by–wave basis, hence the structure was dynamic. However, the net rate of change was small, which means the overall effect of this large gross change (cobble activity) over many waves was small, leading to minimal overall impact on the revetment morphology. This observation is directly comparable to the sandy beach field measurements of Blenkinsopp et al. (2010) who demonstrated that the volume of sediment transported by single waves can be comparable to the net transport which occurs over several hours. This suggests that beaches can be very dynamic over short timescales, but over multiple waves, cross–shore sediment fluxes approximately balance leading to minimal net transport. Here, a large value of the gross volume change rate and a small value of net volume change rate would indicate that the revetment volume fluctuates significantly over short timescales, but that these changes balance out over longer timescales and lead to minimal overall net volume change in a 10 minute period. Section 4.1.3 showed that during runs DR1 to DR4, the gross and net rates of change remain relatively constant with only small changes each time the water level was changed and more of the revetment was exposed to swash processes. There was some evidence that rates of change decreased with time at each water level, regardless of the percentage of overtopping. This suggests that the revetment was approaching an equilibrium

with the wave and water level conditions — this was most evident for run DR4 (Figure 6).

Beyond demonstrating that the transport of cobbles was predominantly landward and hence upward, RFID detection showed a rotational motion of particles within the revetment body. Within the parts of the revetment most strongly influenced by swash motions (toe and lower slope), the instrumented cobbles tended to move seaward by rolling down the slope due to both backwash flows and gravity. Once they reached the active area of the toe and seaward of the toe, they were pushed landward by the uprush and transported onto the structure and over the crest through rollover transport. After further wave actions and mobilisations, cobbles on the upper part of the revetment face became buried by newly transported cobbles, and were eventually exposed as the face of the revetment retreated. It is important to bear in mind that the rollover process can only occur because of the revetment porosity, which yields to a weaker backwash than uprush. This overall rotational motion occurs within the retreating structure, and the combination of gravity and swash effectively induces the overall landward motion.

Accretion of the crest would be expected under rollover transport, particularly as the water level increased and more cobbles were transported onto the crest, however this was counterbalanced by the observed loss of sand from beneath the revetment during the first 28 hours. During DR4, the rate of rollover transport increased due to higher overtopping rates, leading to only a small, 4 cm increase in crest height during this water level increment. While loss of sand is thought to be the major reason for the minimal increase in crest height, van der Meer (1988) and Powell (1990) found that for gravel beaches, a low value of the grading coefficient $D_{85}/D_{15}$ (corresponding to well–sorted material as used here) leads

to a lower crest elevation. During DRE1, DRE2 and DRE3 (energetic conditions of the resilience test), landward cobble transport was significantly intensified (Figure 8). As a result, cobbles were pushed on top of the revetment and beyond (Figure 4g). This suggests that rollover transport may be expected to maintain and indeed increase crest elevation (to keep a positive freeboard) during storm events, particularly if sand loss from beneath the structure is a minor issue as is generally observed in field monitoring of existing composite beaches.

Rollover transport during DR4 and the resilience testing caused an accumulation of material on the revetment crest and a relatively small revetment thickness on the front slope. In response to this, the revetment slope was opportunistically "nourished" by adding an extra 2.50 $m^3$ of cobbles on the front slope, as shown on Figure 11. Following this renourishment, the revetment response was measured for a range of different wave conditions during test series DRN (Table 3). Figure 11a shows the revetment after nourishment and Figure 11b at the end of test series DRN (Table 3). During these tests, the crest retreated by 0.10 m, moving from $x = 262.2$ m to $x = 262.3$ m (Figure 12b). The toe maintained a constant cross–shore position but moved down slightly (Figure 12). However, due to rollover transport onto the crest, the centroid moved 0.47 m landward (Figure 12b) and 0.07 m higher (Figure 12a). The crest elevation increased from $z = 5.46$ m to $z = 5.56$ m, increasing the height of the revetment (Figure 12a). With the extra material, the crest of the revetment increased in overall height due to rollover transport, better maintaining its relative elevation to water level than prior to nourishment. This suggests that the designed volume of the revetment may have been too small, meaning not enough material was available to maintain
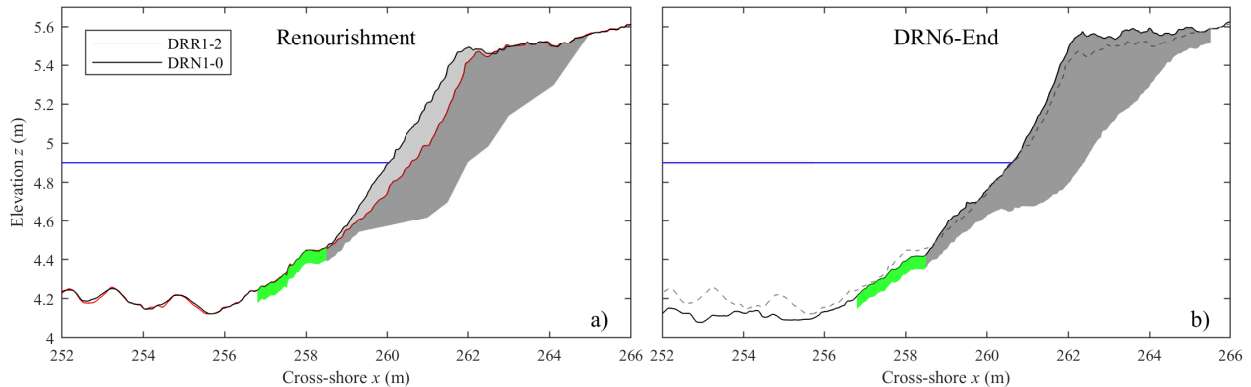
Figure 11: Profile of the dynamic cobble berm revetment after adding an extra 2.50 m$^3$ of identical material (renourishment) and running different wave conditions at 4.9 m water level: (a) the revetment shape after the addition of the extra material to the front slope, DRN1-0; (b) the revetment shape after all the runs (Table 3), DRN6.

the front slope and increase crest elevation due to rollover. It is suggested that the critical mass criteria defined in Ahrens (1990) may be suitable for estimating a minimum stable design volume ($V_d$).

The increase in reflected wave signal over the course of water level increases likely contributed to the local erosion at the toe of the revetment between $x = 253$ m and $x = 258$ m, shown in Figure 3. Similar localised erosion was also observed by Beuzen et al. (2018) in front of a seawall and rubble mound revetment for a rising water level, and interpreted as a transfer of the erosion demand from the sub–aerial beach to the available sand in front of the structure. It is likely that increased wave reflections would lead to more suspended sediment seaward of the revetment toe and in a 3D situation, this sand would become available for longshore transport. However, the total amount of sand available for longshore transport is reduced due to the presence of the revetment which has been shown to retain sand on the subaerial beach.

The presence of the dynamic cobble berm revetment reduced the vertical (Figure 9a) and horizontal (Figure 9b) runup. It was also seen that this reduction was enhanced as the

water level was raised — *e.g.* the horizontal runup was reduced by 2 m during DR1 but by 4 m during DR4. This reduction was likely due to the swash occurring on the porous cobble slope. The measured $R_{2\%}$ (Figure 9a) runup was always smaller than the calculated value of 0.72 m used for the design of the crest elevation using the pure gravel beach formula developed by Poate et al. (2016). This suggests that under the same wave conditions, a beach with a dynamic cobble berm revetment (or a composite beach) is likely to experience smaller runup events than a pure gravel beach (and also a sandy beach). This can be qualitatively explained by the fact that a composite beach is composed of a dissipative sandy surf zone and a reflective, dynamic and porous cobble beach face, whereas a gravel beach has a less dissipative surf zone. At present, no specific runup equation for composite beaches exists, and such an equation is likely to be complicated due to the variability in the position of the cobble berm toe, relative sand and cobble gradients and cobble sizes. Further measurements of runup on composite beaches and dynamic revetments would be beneficial, and aid the development of an approach to estimate wave runup to inform revetment crest elevation design.
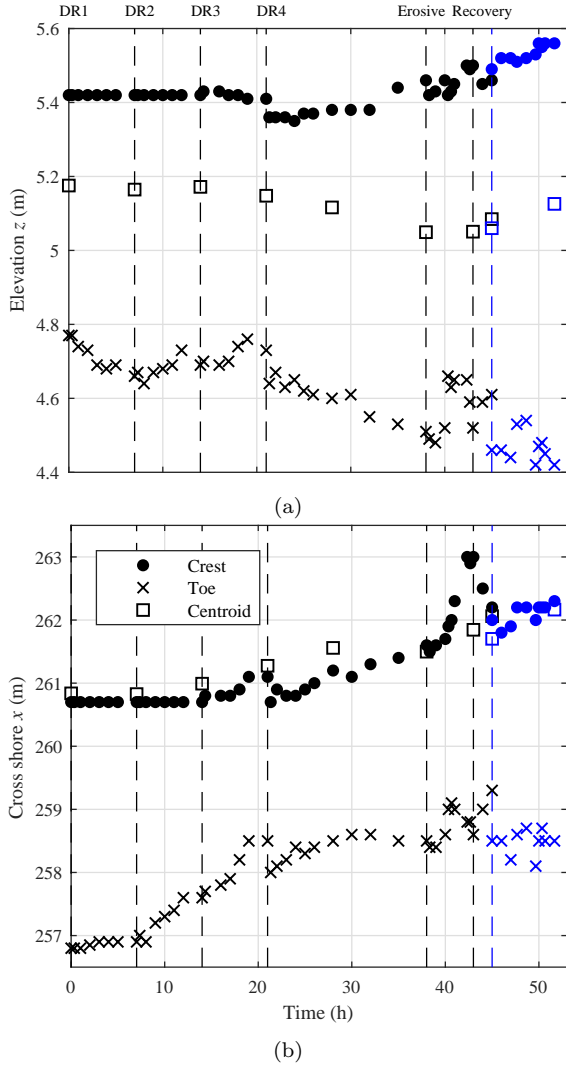
Figure 12: Evolution of the crest, toe and centre of gravity of the revetment through time, in terms of: (a) elevation; (b) cross–shore position. The crest height (dots) is defined as the average of the elevation of the flat area at the top of the revetment. The toe (crosses) is defined as the toe of the cobble body, *i.e.* the seaward limit of the grey area in Figure 4 and Figure 11). The centroid (squares) is defined as the centre of mass of the cobble body. Note that until 45 hours, the data shown in black is identical to that shown in Figure 5 with the extra blue points indicating post–renourishment values. The dashed lines mark the beginning of a new water level (*e.g.* DR1, DR2,...), resilience test cases (*e.g.* erosive and accretive) and the blue dashed line indicates the time of renourishment.

Due to the flat crest of the revetment, the vertical runup height is not considered representative of the extreme swashes (Section 4.3). The horizontal runup limit which is more representative of the swash excursions, was reduced by the presence of the revetment (Figure 9b). Therefore, as the water level increased (*e.g.* during a storm surge) the beach behaved more and more like a composite beach and the runup height was reduced accordingly. It is therefore considered that under increasing water level and energetic wave conditions, the crest (hence the revetment) up–graded to a higher level of protection than it was at before (relative to WL3 for instance). Figure 10a showed that the presence of the revetment slowed down the shoreline retreat as well as the underlying sand interface retreat (the sand is either protected from erosion by the cobbles, or gets deposited by the swash percolating through the cobbles and accumulates within the revetment; further field work is required to fully understand this process). However, differences remain between these two types of retreat and it highlights the fact that the shoreline may not be a suitable parameter to compare the retreat. Figure 10b showed that the sandy beach berm retreated 8 m more than the cobble berm under the same wave energy and water level forcing (Figure 3). It therefore appears that assessing the retreat using the berm position is more appropriate for a dynamic cobble berm revetment. In addition, the berm retreat is directly linked to the horizontal runup excursion shown in Figure 9b (also seen in Figure 3).

Dynamic cobble berm revetments effectively create and artificial composite beach and are characterised by an inherent dynamic stability. The 2D results do not show obvious localised scouring or increase erosion of the sandy component of the beach through cross–shore processes. Beyond the performance of this structure regarding coastal protection, it is impor-

tant to mention that dynamic cobble berm revetments are likely to be low cost structures compared to traditional coastal protection structures, particularly where cobbles can be locally sourced. They do not require any foundation preparation or specialist equipment or expertise for installation which makes them an interesting alternative for developing nations.

## 6. Preliminary design guidelines

The data collected in this experiment are not sufficient to provide complete revetment design guidance. Only one type of material, one revetment position and initial geometry and a narrow range of hydrodynamic conditions were tested. In addition, the 2D nature of the flume experiment limited the analysis to cross–shore processes only. Nevertheless, some basic design suggestions can be drawn from this experiment to be used by practical engineers as the basis for the design of dynamic cobble berm revetments.

The primary objective of a dynamic cobble berm revetment is to limit wave runup and overtopping and to protect the hinterland during extreme storms which are associated with large waves and extreme water levels. For these reasons, dynamic revetments have the potential to provide coastal protection for a wide range of coastlines, ranging from natural habitats to urbanised coasts. The size and volume of the material can be adapted depending on design conditions, from estuaries to open coasts. As observed in the experiment, dynamic revetments do not provide a fixed, hard barrier but evolve and retreat gradually under wave action. As such, any revetment is ideally placed above the natural high tide berm where it will only interact with waves during elevated high tides when waves are relatively large. If sinking of the revetment can be minimised through further research and development, in this configuration the revetment

would be expected to evolve, gradually retreat and self–adapt to sea level through rollover transport. To allow this, some accommodation space is required between the initial position of the revetment and the landward asset to be protected.

The crest elevation is a site–specific parameter which is dependent on the predicted wave runup for a given design wave and water level condition. While no wave runup equation for composite beaches or dynamic revetments currently exists, the work presented here suggests that existing gravel beach runup equations provide an overestimate of wave runup and so could be used for conservative design.

To estimate the minimum revetment volume per unit width, the critical mass criteria developed by Ahrens (1990) for artificial gravel beaches is suggested. However, as this criteria has not been robustly tested for dynamic cobble berm revetments, at least an extra 10 % of material should be added to account for cross–shore losses. It is also necessary to account for losses due to gradients in longshore transport which could be estimated using existing gravel beach longshore transport equations (Kamphuis, 1991; CERC, 1984; Wellen et al., 2000; McCarroll et al., 2019; Tomasicchio et al., 2013, 2015; van Rijn, 2014). Post–construction monitoring of the revetment, combined with estimates of longshore cobble transport should be used to plan cobble renourishments over the life of the revetment.

The results presented here demonstrate that the gradient of the revetment front slope is controlled by the short term wave conditions (Figure 7, Figure 6c). Thus there is no need to carefully design the gradient of the revetment slope. It is recommended simply that sufficient volume is placed in front of the

crest to form the lowest expected gradient based on historical wave steepness data. For conservative design, it is suggested that this volume should be in addition to the critical mass value calculated using Ahrens (1990).

In the experiment, the revetment was placed by dumping stone and then reshaped to the required profile using a front–end loader and manual profiling. It is suggested that a similar process be used in the field and no specialist equipment is necessary. Indeed, as it was observed that wave action will rapidly reshape the revetment to a new profile after a change in wave conditions, it may be sufficient to simply place the required volume of cobbles to achieve the design crest height and minimum revetment slope and then allow wave action to shape the seaward face of the revetment.

Results from pure gravel beaches (van der Meer, 1988; Powell, 1990) suggest that material with a high grading coefficient, $D_{85}/D_{15}$ should lead to a higher crest. This suggests that it may be beneficial to used poorly sorted material with a lower porosity than used in the current experiment. However, at this stage, no conclusion can be drawn regarding the size, type and shape of the material to be used for given design conditions. Future work is needed to study the performance of different cobble sizes, shapes and sorting for varying wave conditions.

## 7. Conclusion

Dynamic cobble berm revetments are inspired by natural composite beaches, and are expected to mimic their behaviour to provide coastal protection. The few existing examples of dynamic cobble berm revetments presented in Section 2.3 motivated the DynaRev large scale laboratory flume experiment, performed at the GWK flume (Germany). Within the limitations of a 2D laboratory flume, this experiment was designed to better understand the be-

haviour of a dynamic cobble berm revetment, and assess its performance as a coastal protection structure under wave attack and a rising water level.

The dynamic cobble berm revetment demonstrated a remarkable dynamic stability, as cobbles within the structure moved with every wave but the global shape of the revetment remained stable with net the rate of bed evolution an order of magnitude lower than the gross rate. Net changes were predominantly localised in the front face of the revetment, mainly due to the underlying erosion of sand caused by the backwash percolating through the structure. The revetment toe, crest and centroid also retreated landward and moved slightly upward under water level rise. This translation was driven by rollover sediment transport which moved more than 70 % of the instrumented cobbles landward. This rollover transport played a major role in maintaining the revetment elevation, while the sand underneath was washed away due to the high porosity of the material used.

The presence of the dynamic cobble berm revetment reduced the shoreline and berm retreat, decreased the amount of sand moving from the sub–aerial to sub–aqueous beach and significantly reduced the vertical and horizontal runup, hence the potential for erosion of the hinterland. Wave reflection was increased by the presence of the revetment, and this played a role in the erosion of sand seaward of the revetment toe.

Based on this experiment, dynamic cobble berm revetments appear to be a sustainable and affordable option for many locations experiencing coastal erosion where complete protection from coastal hazards is not needed and some coastal retreat is acceptable — *i.e* accommodation space available. Some basic design guidelines are provided as a first step for practical engineers to design dynamic cobble berm revetments. Nevertheless, further research into composite beach and dynamic revetments

needs to be done before comprehensive guidance can be provided. Future work includes development of a numerical model that can predict revetment behaviour, field experiments at composite beaches and dynamic revetment sites including measurements of longshore cobble movement, and investigation of different material types, sizes and grading.

**Acknowledgements**

**References**

Ahrens, J. P. (1990). Dynamic revetment. *Coastal Engineering*, *138*, 1837–1850.

Allan, J. C., & Gabel, L. L. (2016). *Monitoring the response and efficacy of a dynamic revetment constructed adjacent to the columbia river south jetty, Clatsop county, Oregon.*. Technical Report O-16-07 Oregon Department of Geology and Mineral Industries.

Allan, J. C., Geitgey, R., & Hart, R. (2016). Dynamic revetments for coastal erosion stabilization: a feasible analysis for application on the oregon coast. *Oregon Department of Geology and Mineral Industries*, *Special issue, 37*.

Allan, J. C., Harris, E., Stephensen, S., Politano, V., Laboratory, H., Folger, C., & Nelson, W. (2012). *Hatfield Marine Science Center Dynamic Revetment Project*. Technical Report Hatfield Marine Science Center, Oregon State University.

Allan, J. C., Hart, R., & Tranquili, J. V. (2006). The use of passive integrated transponder (pit) tags to trace cobble transport in a mixed sand-and-gravel beach on the high-energy oregon coast, usa. *Marine Geology*, *232*.

Allan, J. C., & Komar, P. (2004). Environmentally compatible berm and artificial dune for shore protection. *Shore and Beach*, *721*, 9–16.

Almeida, L. P., Masselink, G., Russel, P. E., & Davidson, M. A. (2015). Observations of gravel beach dynamics during high energy wave conditions using a laser scanner. *Geomorphology*, *228*, 15–27.

Beuzen, T., Turner, I. L., Blenkinsopp, C. E., Atkinson, A., Flocard, F., & Baldock, T. E. (2018). Physical model study of beach profile evolution by sea level rise in the presence of seawalls. *Coastal Engineering*, *136*, 172–182.

Blenkinsopp, C. E., Bayle, P. M., Conley, D., Masselink, G., Gulson, E., Kelly, I., Ganderton, P., Almar, R., Turner, I. L., Baldock, T. E., Beuzen, T., McCall, R. T., Renier, A., Troch, P., Sanchez, D. G., Hunter, A., Bryan, O., Hennessey, G., McCarroll, J., Barrett, A., Schimmels, S., & Kudella, M. (In review). High-resolution, prototype-scale laboratory measurements of nearshore wave processes and morphological evolution of a sandy beach and dynamic cobble berm revetment. *Scientific Data*, .

Blenkinsopp, C. E., Mole, M. A., Turner, I. L., & Peirson, W. L. (2010). Measurements of the time-varying free-surface profile across the swash zone obtained using an industrial lidar. *Coastal Engineering*, *57*, 1059–1065.

Cartwright, A., Brundrit, G., & Fairhurst, L. (2008). *Global Climate Change and Adaptation A Sea-Level Rise Risk Assessment*. Technical Report LaquaR Consultant CC Cape Town, South Africa.

CERC (1984). *Shore Protection Manual* volume 2. (4th ed.). U.S. Government Printing Office, Washington, D.C.: U.S. Army Waterways Experiment Station.

Dean, R. G. (1973). Heuristic models of sand transport in the surf zone. In *Engineering Dynamics in the Surf Zone. N.S.W, Sydney* (pp. 208–214).

Dean, R. G., & Dalrymple, R. A. (2002). Coastal processes with engineering applications. chapter 3. (pp. 35–65). Cambridge University Press.

DeConto, R. M., & Pollard, D. (2016). Contribution of antarctica to past and future sea-level rise. *Nature*, (pp. 591–597).

Downie, K. A., & Saaltink, H. (1983). An artificial cobble beach for erosion control. In *Coastal Structure '83* (pp. 846–859). Reston, Va., American Society of Civil Engineers.

Everts, C. H., Eldon, C. D., & Moore, J. (2002). Performance of cobble berm in southern california. *Shore and Beach*, *70⁄4*, 4–14.

French, P. W. (2001). Coastal defences : processes, problems and solutions. chapter 12. (pp. 311–325). London: London : Routledge.

van Gent, M. R. A. (2010). Dynamic cobble beaches as sea defence. In *Proceedings of the Third International Conference on the Application of Physical Modelling to Port and Coastal Protection, Barcelona.*.

Gourlay, M. R. (1968). *Beach and Dune Erosion Tests*. Technical Report M935/M936 Delft Hydraulic Laboratory, the Netherlands.

van Hijum, E. (1976). Equilibrium profiles and longshore transport of coarse material under oblique wave attack. *Coastal Engineering*, *74*, 1258–1276.

van Hijum, E., & Pilarczyk, K. W. (1982). *Equilibrium Profile and Longshore Transport of Coarse Material Under Regular and Irregular Wave Attack*. Publication (Waterloopkundig Laboratorium (Delft, Netherlands)). Delft Hydraulics Laboratory.

Howe, D., & Cox, R. (2018). Upgrading breakwaters in response to sea level rise: practical insights from physical modelling. In *Proceedings of the 36th International Conference*.

Hudson, T., Keating, K., & Pettit, A. (2008). *Delivering benefits through evidence. Coast estimation for coastal protection - summary of evidence*. Technical Report SC080039/R7 Environmental agency Environment Agency, Horizon House, Deanery Road, Bristol, BS1 5AH.

Jennings, R., & Schulmeister, J. (2002). A field based classification scheme for gravel beaches. *Marine Geology*, *186*, 611–228.

Johnson, C. N. (1987). Rubble beaches versus revetments. In *Coastal Sediments '87* (pp. 1217–1231). Reston, Va., American Society of Civil Engineers.

Kamphuis, J. W. (1991). Alongshore sediment transport rate. *Journal of Waterway, Port, Coastal and Ocean Engineering*, *117*, 624–640.

Kirk, R. M. (1992). Experimental beach reconstruction-renourishment on mixed sand and gravel beaches, washdyke lagoon, south canterbury, new zealand. *Coastal Engineering*, *17*, 253–277.

Komar, P., & Allan, J. C. (2010). Design with nature strategies for shore protection - the construction of a cobble berm and artificial dune in an oregon state park. In *Puget Sound Shorelines and the Impacts of ArmoringProceedings of a State of the Science Workshop* (pp. 117–126). U.S. Geological Survey Scientific Investigations Report 2010-5254.

Loman, G. J. A., van Gent, M. R. A., & Markvoort, J. W. (2010). Physical model testing of an innovative cobble shore, part i: Verification of cross-shore profile deformation. In *Third International Conference on the Application of Physical Modelling to Port and Coastal Protection*.

Lorang, M. S. (1991). An artificial perch-gravel beach as a shore protection structure. In *Coastal Sediments '91* (pp. 1916–1925). Reston, Va., American Society of Civil Engineers volume 2.

McCall, R., Rijper, H., & Blenkinsopp, C. (2019). Towards the development of a morphological model for composite sand-gravel beaches. In *Coastal Sediment 2019* (pp. 1889–1900).

McCarroll, R. J., Masselink, G., Wiggins, M., Scott, T., Billson, O., Conley, D. C., & Valiente, N. G. (2019). High efficiency gravel longshore sediment transport and headland bypassing over an extreme wave event. *Earth Surface Processes and Landforms*, *0*.

van der Meer, J. W. (1988). *Rock slopes and gravel beaches under wave attack.*. Ph.D. thesis University of Technology, Delft.

van der Meer, J. W., & Pilarczyk, K. W. (1986). Dynamic stability of rock slopes and gravel beaches. *Coastal Engineering*, *125*, 1713–1726.

Pilarczyk, K. W., & Boer, K. D. (1983). *Stability and profile development of coarse material and their application in coastal engineering*. Technical Report Delft Hydraulics.

Poate, T. G., McCall, R. T., & Masselink, G. (2016). A new parameterisation for runup on gravel beaches. *Coastal Engineering*, *117*, 176–190.

Powell, K. A. (1988). The dynamic response of shingle beaches to random waves. *Coastal Engineering*, *130*, 1763–1773.

Powell, K. A. (1990). *Predicting Short Term Profile response for shingle beaches.*. Technical Report SR 219 HR Wallingford, Oxfordshire, UK.

Powell, K. A. (1993). *Dissimilar Sediments: Model tests of replenished beaches using widely graded sediments*. Technical Report SR 250 HR Wallingford.

van Rijn, L. C. (2014). A simple general expression for longshore transport of sand, gravel and shingle. *Coastal Engineering*, *90*, 23–39.

Roman-Blanco, B. L. D. S., Coates, T. T., Holmes,

P., Chadwick, A. J., Bradbury, A., Baldock, T. E., Pedrozo-Acuna, A., Lawrence, J., & Grne, J. (2006). Large scale experiments on gravel and mixed beaches: experimental procedure, data documentation and initial results. *Coastal Engineering*, *53*, 349–362.

Seymour, R. J., Bockstael, N. E., Campbell, T. J., Dean, R. G., Komar, P. D., Pilkey, O. H., Pratt, A. P., Snow, M. R., van Dolah, R. F., Weggel, J. R., & Wiegel, R. L. (1995). Beach nourishment and protection. chapter 5. (pp. 107–126). Washington, DC: The National Academies Press.

Sorensen, R. M. (2006). *Basic coastal engineering*. (3rd ed.). New York, London : Springer.

Tomasicchio, G. R., D'Alessandro, F., Barbaro, G., & Malara, G. (2013). General longshore transport model. *Coastal Engineering*, *71*, 28–36.

Tomasicchio, G. R., D'Alessandro, F., Barbaro, G., Musci, E., & Giosa, T. M. D. (2015). Longshore transport at shingle beaches: An independent verification of the general model. *Coastal Engineering*, *104*, 69–75.

Tomasicchio, G. R., D'Alessandro, F., & Musci, E. (2010). A multi-layer capping of a coastal area contaminated with materials dangerous to health. *Chemistry and Ecology*, *26*, 155–168.

Tomasicchio, G. R., Lamberti, A., & Guiducci, F. (1994). Stone movement on a reshaped profile. In *Proceedings of the 24th International Conference on Coastal Engineering. ASCE, Kobe.* (pp. 1625–1640).

Turner, I. L., Russel, P. E., & Butt, T. (2008). Measurement of wave-by-wave bed-levels in the swash zone. *Coastal Engineering*, *55*, 1237–1242.

Ward, D. L., & Ahrens, J. P. (1992). *Laboratory study of a dynamic berm revetment*. Technical Report US Army Corps of Engineers.

Weiner, H. M., Kaminsky, G. M., Hacking, A., & McCandless, D. (2019). *North Cove Dynamic Revetment Monitoring: Winter 2018-2019*. Technical Report 19-06-008 Shorelands and Environmental Assistance Program, Washington State Department of Ecology, Olympia, WA.

Wellen, E. V., Chadwick, A. J., & Mason, T. (2000). A review and assessment of longshore sediment transport equations for coarse grained beaches. *Coastal Engineering*, *40*, 243–275.